

Volume 4, Issue 7 — July-December 2017

E
C
O
R
F
A
N

Journal - Ecuador

ISSN-On line: 1390-9959

ECORFAN[®]



Indexing

- Google Scholar
- Research Gate
- REBID
- Mendeley
- RENIECYT

ECORFAN-Ecuador

Directory

CEO

RAMOS-ESCAMILLA, María. PhD

CAO

OLIVES-MALDONADO, Carlos. MsC

Director of the Journal

PERALTA-CASTRO, Enrique. MsC

Institutional Relations

IGLESIAS-SUAREZ, Fernando. BsC

Editing Logistics

SERRUDO GONZALES- Javier, BsC

Designer Edition

SORIANO-VELASCO, Jesus. BsC

ECORFAN Journal-Ecuador, Volume 4, Issue 7, July-December -2017, is a journal edited six- monthly by ECORFAN. 18 Marcial Romero avenue, Postcode: 241550. Salinas 1 – Santa Elena WEB: www.ecorfan.org/ecuador, journal@ecorfan.org. Editor in Chief: RAMOS-ESCAMILLA, María. PhD, ISSN- On line: 1390-9959. Responsible for the latest update of this number ECORFAN Computer Unit. ESCAMILLA-BOUCHÁN, Imelda. PhD, LUNA-SOTO, Vladimir. PhD, 18 Marcial Romero avenue, Postcode: 241550. Salinas 1 – Santa Elena, last updated December 31, 2017.

The opinions expressed by the authors do not necessarily reflect the views of the editor of the publication.

It is strictly forbidden to reproduce any part of the contents and images of the publication without permission of the National Institute of Copyright.

Editorial Board

NUÑEZ-SELLES, Alberto. PhD

Universidad Evangelica Nacional, Dominican Republic

CHEW-HERNANDEZ, Mario Luis. PhD

University of Nottingham, England

QUINTANA-JARDINES, Ibrahim. PhD

Instituto Nacional de Higiene, Epidemiologia y Microbiologi), Cuba

ESCOBEDO-BONILLA, Cesar Marcial. PhD

Universidad de Gante, Belgium

GARCIA-de SOTERO, Dora Enith. PhD

Universidad de Sao Paulo, Brazil

SANTILLANO-CAZARES, Jesus. PhD

Oklahoma State University, USA

CASTRO-ESPINOSA, Jobany. MsC

Universidad del Valle, Colombia

MARTINEZ-MADRID, Miguel. PhD

University of Cambridge, England

PEREZ-y PERAZA, Jorge. PhD

Centre National de Recherche Scientifique, France

GONZALEZ-ALVARADO, Juan Manuel. PhD

Universidad Politecnica de Madrid, Spain

AVENDAÑO-ARRAZATE, Carlos Hugo. PhD

Universidad de Lleida, Spain

MENDEZ-MEDINA, Ruben Danilo. PhD

University of Bristol, England

ESCAMILLA-GARCIA, Erandi. PhD

University of Burgundy, France

FERNANDEZ-PALACIN, Fernando. PhD

Universidad de Cadiz, Spain

CARBAJAL-de la TORRE, Georgina. PhD

Université des Sciences de Lille 1 France

Arbitration Committee

VM, PhD

ESIQIE – IPN, México

MVHG, PhD

Instituto Politécnico Nacional, México

PRJF, PhD

CINVESTAV-IPN, Mexico

MRM, PhD

Escuela Nacional de Ciencias Biológicas-IPN, Mexico

GOH, PhD

Facultad de Química, UNAM Mexico

AMAJ, PhD

Universidad de Carabobo Venezuela

LPC, BsC

Universidad Juárez Autónoma de Tabasco, Mexico

SMCJ, PhD

Universidad Autónoma Benito Juárez de Oaxaca Mexico

MRMA, MsC

Universidad Nacional Experimental Politécnica de la Fuerza Armada Bolivariana, Venezuela

AMFR, PhD

Instituto Nacional de Pediatría Mexico

PGR, PhD

Institut National Polytechnique de la Lorraine, Francia

RAG, PhD

Universidad de Guanajuato, Mexico

RVH, PhD

Universidad de Guadalajara, Mexico

SSVE, PhD

Universidad Nacional de la Amazonia Peruana, Peru

CSA, PhD

Secretaria de Salud, Mexico

HMR, PhD

University of California, USA

PPI, PhD

Universidad Autonoma de Tamaulipas, Mexico

PNPI, PhD

Instituto Nacional de Neurologia y Neurocirugia, Mexico

DAJWC, PhD

Federal University of Mato Grosso, Brazil

PRCC, PhD

Universidad Central de Venezuela, Venezuela

DLFSNM, PhD

Universidad Autonoma de Coahuila, Mexico

RLR, PhD

DLFA,. PhD

Universidad Autonoma de Sonora, Mexico

CBMT, PhD

Universidad Autonoma de Baja California, Mexico

HGV, BsC

Instituto Nacional de Higiene y Epidemiologia, Cuba

EZNG, PhD

Instituto Nacional de Cardiologia, Mexico

Presenttion

ECORFAN Journal-Ecuador is a research journal that publishes articles in the areas of:

Experimental design **C**ommerce **O**ptions **R**ural **F**lora and Fauna **A**gronomy **N**atural.

In Pro-Research, Teaching and Training of human resources committed to Science. The content of the articles and reviews that appear in each issue are those of the authors and does not necessarily the opinion of the editor in chief.

As a first article we present, *Energy potential of some forest species in the northern zone of the Yucatan Peninsula, for their use as solid fuels*, by AGUILAR-SÁNCHEZ, Patricia, CARRILLO-ÁVILA, Noel, SUÁREZ-PATLÁN, Edna Elena, ORDÓÑEZ-PRADO, Casimiro, as the following chapter we present, *The ferrite nanoparticles (Fe₂O₃) impact on germination, growth and lignine content of carrot (Daucus carota)*, by VALLE-GARCIA, Jessica Denisse, VAZQUEZ-NUÑEZ, Edgar and CASTELLANO-TORRES, Laura Edith, with ascription in Universidad de Guanajuato, as next chapter we present, *Synthesis and characterization of Pd / TiO₂ thin films with possible applications in photocatalysis*, by TIRADO-GUERRA, Salvador and VALENZUELA-ZAPATA, Miguel, as the following chapter we present, *Renewable energy potential in the Usumacinta watershed: Status and opportunities*, by PAMPILLÓN-GONZÁLEZ Liliana, SARRACINO-MARTÍNEZ Omar, HERNÁNDEZ-GÁLVEZ Geovanni, ORDAZ-FLORES Alejandro, with secondment in the Universidad Juárez Autónoma de Tabasco and Universidad Iberoamericana, as a last article we present, *Lectins Gal / GalNAc from medicinal plants extracts with gastrointestinal activity have effects on the biological activity of Escherichia Coli O157H7*, by GILES-RIOS, Héctor, COUTIÑO-RODRIGUEZ, Rocío, ARROYO -HELGUERA, Omar, HERNÁNDEZ-CRUZ, Pedro, with secondment at Universidad Veracruzana and Research Center of the UNAM-UABJO School of Medicine, Oaxaca School of Medicine.

Content

Article	Page
Energy potential of some forest species in the northern zone of the Yucatan Peninsula, for their use as solid fuels AGUILAR-SÁNCHEZ, Patricia, CARRILLO-ÁVILA, Noel, SUÁREZ-PATLÁN, Edna Elena, ORDÓÑEZ-PRADO, Casimiro	1-7
The ferrite nanoparticles (Fe₂O₃) impact on germination, growth and lignine content of carrot (<i>Daucus carota</i>) VAZQUEZ-NUÑEZ, Edgar, VALLE-GARCIA, Jessica Denisse and CASTELLANO-TORRES, Laura Edith	8-14
Synthesis and characterization of Pd/TiO₂ thin films with possible applications in photocatalysis TIRADO-GUERRA, Salvador & VALENZUELA-ZAPATA, Miguel	15-25
Renewable energy potential in the Usumacinta watershed: Status and opportunities PAMPILLÓN-GONZÁLEZ Liliana, SARRACINO-MARTÍNEZ Omar, HERNÁNDEZ-GÁLVEZ Geovanni, ORDAZ-FLORES Alejandro	26-44
Lectins Gal/GalNAc from medicinal plants extracts with gastrointestinal activity have effects on the biological activity of <i>Escherichia Coli</i> O157H7 GILES-RIOS, Héctor, COUTIÑO-RODRIGUEZ, Rocío, ARROYO-HELGUERA, Omar, HERNÁNDEZ-CRUZ, Pedro	45-59

Instructions for Authors

Originality Format

Authorization Form

Energy potential of some forest species in the northern zone of the Yucatan Peninsula, for their use as solid fuels

AGUILAR-SÁNCHEZ, Patricia*†, CARRILLO-ÁVILA, Noel, SUÁREZ-PATLÁN, Edna Elena, ORDÓÑEZ-PRADO, Casimiro

Received July 18, 2017; Accepted November 5, 2017

Abstract

Campeche, Quintana Roo and Yucatan are states that have high forest activity, in tropical forest and wood industry, with a great waste disposal, which could be an alternative for profitable use. Promoting the management and use of this biomass, would generate energy benefits for the North of the Yucatan Peninsula. In this work, the energy potential of wood residues generated in the states of Campeche, Quintana Roo and Yucatán was determined by the calorific value and basic density. The wood preparation for density and calorific value studies was carried out in accordance with the Tappi T264 standard. The heat value was determined with a PARR 1266 calorimeter and the basic density according to the Tappi T258 standard. The statistical analysis was developed with the SAS program, version 9.3. The results show significant differences for basic density and heat value, being *Bucida buceras L.* the species with the highest values in both parameters, however, in this work was a negative correlation between the basic density and the calorific value.

Heat value, basic density, Yucatan peninsula, Wood waste

Citation: AGUILAR-SÁNCHEZ, Patricia, CARRILLO-ÁVILA, Noel, SUÁREZ-PATLÁN, Edna Elena, ORDÓÑEZ-PRADO, Casimiro. Energy potential of some forest species in the northern zone of the Yucatan Peninsula, for their use as solid fuels. ECORFAN Journal-Ecuador. 2017, 4-7:1-7

*Correspondence to Autor (E-mail: aguilar.patricia@inifap.gob.mx)

† Researcher contributing as first author.

1 Introduction

The energy system of a country is fundamental for its economic, environmental and social development, where a sustainable energy supply allows an adequate functioning of the productive system and, as a consequence, provides social benefits through the generation of jobs (Kautto N. and Peck P., 2012, Bondolich C. and Roccia H., 2013). In Mexico, there is potential for the generation of alternative energies from biomass, however, in 2010 the participation of this in the energy supply was only 4.3%, mainly due to the use of firewood and cane bagasse (García et al., 2015).

The northern zone of the Yucatan Peninsula is one of the areas with the greatest potential for the use of wood energy, with a great diversity of forest species, characteristic of the region. Much of the forest management practiced in the area focuses on the use of precious woods such as red cedar and mahogany, however, many of the species that coexist in the area are the main source of energy use, used as firewood for the rural populations of Campeche, Quintana Roo and Yucatán. Although there is a commercial use for their wood, the forestry activity and the wood industry generate a large amount of waste in the form of sawdust and some other pieces of wood of different shapes, which could represent greater income opportunities if they were used as energy options. (UNDP et al., 2014; German-Nava et al., 2014).

Therefore, within a sustainable scenario, biomass hopes to become one of the best renewable resources for the production of food, livestock feed, materials, chemicals, fuels, energy and heat (Aresta, 2012, García et al., 2015). In addition, studies prove that the chemical composition of natural biomass is simpler than that of solid fossil fuels, however, the characteristics of the biomass vary according to the source and need to be known in detail before any thermochemical process is developed. (Sauciuc et al., 2014; Vassilev et al., 2010).

It is said that the biomass potential represents a significant amount of energy and there are several transformation processes, which can be used to produce energy in the form of gas, liquid and solid, from virgin or residual biomass, and the potential characteristics of these Raw materials such as moisture and energy content are considered important effects for the selection of species and biomass residues (Klass et al., 1998, Ramírez, 2015). Thus, energy options such as solid fuels are seen as one of the best options, since this biomass does not need any prior chemical intervention for its use, besides having environmental and economic advantages, since it is cheap and is a renewable resource (Erol et al., 2010).

The calorific power of the biomass is an indicator of the energy that is chemically bound to it and that in the combustion process is transformed into thermal energy. The calorific value is considered the most important property of a fuel, since it determines its energetic value (Erol et al., 2010). Previous studies mention that the range of calorific power for wood is from 4000 to 5000 kcal · kg⁻¹ in dry weight (Tancredi et al., 2005). On the other hand, density is a variable linked to physical properties, which has a positive correlation with calorific value (Kumar et al., 2010). Some of the values reported for densities range from 440 to 963 kg · m⁻³ (Manulala and Meincken, 2009, Telmo and Lousada, 2011).

However, due to the growing demand for energy, limitations for the creation of new technologies from biomass, have made fossil fuels with high calorific value widely used, making biomass lose importance despite the recent development of systems for the production of cleaner energy (Cutz et al., 2016, Bilgili et al., 2017).

So in this work the energy potential of wood residues generated in the states of Campeche, Quintana Roo and Yucatan was determined by determining the calorific value and basic density, to determine their viability as solid fuels.

2. Methodology

To achieve the stated objective, the following methodology was followed: Wood samples were collected from the main species harvested in the felling areas of the timber management programs of the states of Campeche, Quintana Roo and Yucatán. The samples taken were of residues that are generally abandoned in the field as branches of different diameters and pieces that are not sent to the transformation centers. Each sample collected was labeled with basic control information: name and coordinates of the site, date, species and sample number. These samples were sent to the laboratory of forest products and wood technology of the San Martinito Experimental Field (INIFAP), for the estimation of the basic density and calorific value.

Preparation of simple

The collected materials were transported to the laboratory where the samples were prepared in accordance with the TAPPI T257 standard. The milling of the study material was done using a Thomas Wiley mill. The milled material was sieved with No. 40 and 60 meshes, using only the material retained in No. 60 mesh. This material was placed in paper bags with their respective identification and stored for later calorimetry analysis.

Heating power (PC)

For the PC determination, a Parr 1266 Calorimeter was used, following the procedure of the operation manual. The calorimeter was calibrated with benzoic acid tablets of calorific grade. For its determination, a pellet was formed with the ground material with a weight between 0.5 to 0.9 g, with a sample moisture content between 5-10%. The pellet was placed in a combustion pod, in addition to the 10 cm ignition wire on the pellet, preventing the wire from rubbing against the walls of the capsule.

Then, the capsule with the pellet and the wire were placed inside the oxygen pump, closing to inject as oxygen the combustion medium. Finally, the pump was placed inside a bucket and connected to the electrodes. The determination of the CP was carried out in a time not greater than ten minutes, performing five repetitions per sample. The results were obtained directly from the calorimeter in units $\text{cal} \cdot \text{g}^{-1}$ and adjusted according to equation 1.

$$PCt = \frac{Ee(At) - 10 - Lai(k)}{Pm} \quad (1)$$

Where:

PCt total calorific value [$\text{cal} \cdot \text{g}^{-1}$]

The equivalent energy [$\text{cal} \cdot ^\circ\text{C}^{-1}$]

At increase in temperature [$^\circ\text{C}$]

The length of the burned ignition wire [cm]

Constant k (2.3 $\text{cal}\cdot\text{cm}^{-1}$)

Pm weight of the wood pellet [g]

Density

The density of the wood was determined by the volumetric displacement method, since precision and reliability were required in the results and the pieces collected from wood were irregularly shaped, for this purpose wax was used to cover the samples and avoid measurement errors. the weight of the sample before and after waxing. Afterwards, the sample was introduced in a container with water until it was completely covered. The container was placed on the digital balance so that during the operation the weight of the displaced liquid was recorded directly, which is proportional to the force of the water on the sample. The density of water is equal to $1 \text{ g} \cdot \text{cm}^{-3}$ and therefore the weight recorded by the balance is equal to the volume of the sample. The basic density was calculated by relating the anhydrous mass and volume of the saturated wood, as shown in equation 2.

$$Db = \frac{Po}{Vv} \quad (2)$$

Where:

Db basic density of wood [kg · m⁻³]

Po anhydrous weight [kg]

Vv green volume [m³]

With the weight and volume data, the initial moisture content was calculated, expressed in the equation 3:

$$CH = \frac{(Ph - Po)}{Po} \cdot 100 \quad (3)$$

Where:

CH moisture content [%]

Ph initial weight of wet wood [kg]

Po anhydrous weight [kg]

For the estimation of the basic density and calorific power, five repetitions were made for each species and place of origin of the sample. An analysis of variance was performed represented in the statistical model of equation 4, as well as a multiple comparison of means by the Duncan method, using the SAS 9.3 program®.

$$y_{ij} = \mu + \tau_i + e_{ij} \quad (4)$$

Where:

Y_{ij} is the answer

μ is the general average of the experiment

τ_i is the effect of the treatment

e_{ij} is the treatment error associated with the response Y_{ij}

3. Results

According to the multiple means comparison, statistically there are significant differences in calorific power and basic density with p < 0.05 of the species studied. In relation to the calorific value (table 1) 11 groups were obtained, in a range of values ranging from 4000.3 to 4706.71 kcal · kg⁻¹ being the species *Coccoloba spicata* (Bo'o) with lower PC and *Bucida buceras* L. (Pucte) the one with the highest PC value.

The basic density of the studied species was presented in values of 366.8 kg · m⁻³ and 846.2 kg · m⁻³ (table 2), being the species *Bursera simaruba* Sarg. (Chaká) the lightest wood and *Bucida buceras* L. (Pucte) the densest.

It can be observed that the calorific value and density results are in accordance with the data reported in the literature, noting that *Bucida buceras* L. and *Psychotria pubescens* Swartz were the species with the highest combustion values, having an energy content per unit volume of 3999.58 and 3914.72 Mcal · m⁻³ respectively.

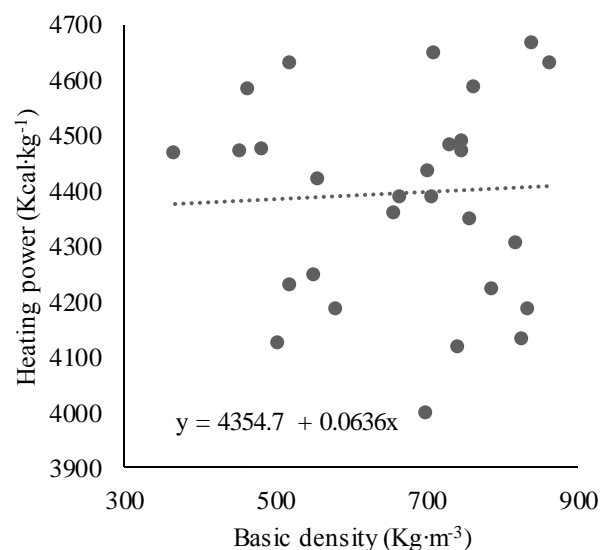
Species	Calorific power (kcal·kg ⁻¹)
<i>Bucida buceras</i> L.	4706.71 A
<i>Psychotria pubescens</i> Swartz	4667.61 AB
<i>Lonchocarpus castilloi</i> Standl.	4649.35 AB
<i>Lysiloma latisiliquum</i> (L.) Benth.	4631.77 AB
<i>Thouinia pausidentata</i>	4588.67 B
<i>Swietenia macrophylla</i> King.	4585.65 B
<i>Swartzia cubensis</i> (Britt & Wils.) Standl.	4490.52 C
<i>Matayba oppositifolia</i> Britton	4483.28 CD
<i>Tectona grandis</i>	4473.81 CD
<i>Vitex gaumeri</i> Greenm.	4470.84 CD
	4470.58 CD
<i>Psidium sartorianum</i> (Berg.) Ndzu.	4467.89 CD
<i>Bursera simaruba</i> Sarg.	4434.65 CDE
<i>Exostema caribaeum</i> (Jacq) Roem. & Schult.	4421.45 CDE
<i>Piscidia piscipula</i> (L) Sarg	4390.70 CDEF
<i>Gymnopodium floribundum</i> Roste	4388.82 DEF
<i>Platymiscium yucatanum</i> Standl	4360.13 EF
<i>Diospyros cuneata</i> Stanley	4350.90 EF
<i>Caesalpinia violacea</i> (Miller) Standl.	4304.48 FG
<i>Mimosa bahamensis</i> Benth	4247.24 GH
<i>Thevetia gaumeri</i> hemsl	4231.46 GH
<i>Lysiloma latisiliquum</i> (L.) Benth.	4222.46 GHI
<i>Acacia gaumeri</i> Blake	4187.20 HIJ
<i>Guetta combsii</i> Urban	4186.27 HIJ
<i>Caesalpinia gaumeri</i> Greenm.	4131.82 IJ
<i>Acacia milleriana</i> Standl.	4124.52 J
<i>Guazuma ulmifolia</i> Lam.	4118.19 J
<i>Lonchocarpus</i> Rugosa	4000.30 K

Table 1 Average calorific value of the forest residues of the Yucatan Peninsula (values with the same letter are not significantly different)

Species	Density (kg·m ⁻³)	
Bucida buceras L.	846.2	A
Psychotria pubescens Swartz	838.7	B
Caesalpinia gaumeri Greenm.	834.6	C
Acacia milleriana Standl	825.6	D
Mimosa bahamensis Benth	817.9	E
Acacia gaumeri Blake	785.6	F
Thouinia pausidentata	763.2	G
Caesalpinia violacea (Miller) Standl.	756.4	H
Swartzia cubensis (Britt & Wils.) Standl.	747.1	I
Psidium sartorianum (Berg.) Ndzu.	746.8	J
Lonchocarpus Rugosa	742.1	K
Matayba oppositifolia Britton	730.9	L
Lonchocarpus castilloi Standl.	710.9	M
Platymiscium yucatanum Standl.	707.4	N
Exostema caribaeum (Jacq) Roem. & Schult.	700.9	O
Coccoloba spicata	698.3	P
Gymnopodium floribundum Roste	665.4	Q
Diospyros cuneata Stanley	657.1	R
Guettia combsii Urban	580.1	S
Piscidia piscipula (L) Sarg	555.7	T
Thevetia gaumeri hemsl	550.1	U
Lysiloma latisiliquum (L.) Benth.	520.4	V
Guazuma ulmifolia Lam.	503.0	W
Tectona grandis	483.0	X
Swietenia macrophylla King.	463.1	Y
Vitex gaumeri Greenm.	452.7	Z
	366.8	A

Table 2 Average basic density of the forest residues of the Yucatan Peninsula (values with the same letter are not significantly different)

The forest residues evaluated in this work show a coefficient of determination R² of 0.002, which indicates that the values of basic density and calorific value are not directly related (figure 1), as was the species *Lysiloma latisiliquum* (L.) Benth, from which samples were obtained from the states of Campeche and Quintana Roo, these had an equal basic density, however, the calorific value was different, being higher the species from Quintana Roo.



Graphic 1 Linear regression analysis, calorific value & basic density

4. Conclusions

Forest residues from forest management programs in the northern Yucatan Peninsula represent an opportunity for the generation of alternative energies. Given that, the values of calorific power and basic density obtained in this study showed high values such as the species *Bucida buceras* L. (Pucte).

On the other hand, the viability of forest biomass as fuel depends on the correlations and associations between its chemical composition, so it is important to have other analyzes such as chemical composition and elemental and proximal analysis that can strengthen this study.

Acknowledgement

The authors thank the Sector Fund CONACYT / CONAFOR 116375 for supporting the development of this research.

5. References

- Alemán-Nava, G. S., Casiano-Flores, V. H., Cárdenas-Chávez, D. L., Díaz-Chavez, R; Scarlet, N., Mahlknecht, J., Dallemand, J. F., Parra, R. (2014). Renewable energy research progress in Mexico: A review. *Renewable and Sustainable Energy Reviews*, 32, pp.140–153.
- Aresta, M., Dibenedetto, A., Dumeignil, F. (2012). Biorefinery from biomass to chemicals and fuels. De Gruyter, Alemania.
- Bilgili, F., Koçak, E., Bulut, Ü., Kuşkaya, S. (2017). Can biomass energy be an efficient policy tool for sustainable development? *Renewable and Sustainable Energy Reviews*, 71, pp. 830–845.
- Bondolich, C., Rocca, H. (2013). Desarrollo regional con energía de la biomasa Fundación Agropecuaria para el Desarrollo de Argentina, p.14.
- Cutz, L., Haroc, P., Santana, D., Johnsson, F. (2016). Assessment of biomass energy sources and technologies: The case of Central America. *Renewable and Sustainable Energy Reviews*, 58, pp. 1411–1431.
- Disponible en: www.ccmss.org.mx/wp-content/uploads/2014/10/CATALOGO-MADERA.pdf
- Erol, M., Haykiri-Acma, H., Küçükbayrak, S. (2010). Calorific value estimation of biomass from their proximate analyses data. *Renewable energy*, 35, pp. 170-173.
- García, C. A., Riegelhaupt, E., Ghilardi, A., Skutsch, M., Islas, J., Manzini, F., Masera, O. (2015). Sustainable bioenergy options for Mexico: GHG mitigation and costs. *Renewable and Sustainable Energy Reviews*, 43, pp. 545-552.
- Kautto, N., Peck, P. (2012). Regional biomass planning- Helping to realize national renewable energy goals? *Renewable Energy*, 46, pp. 23-30.
- Klass-Donald, L. (1998). Biomass for renewable energy, fuels and chemicals. Academic Press, San Diego California EUA.
- Kumar, R., Pandey, K.K., Chandrashekar, N., Mohan, S. (2010). Effect of tree-age on calorific value and other fuel properties of Eucalyptus hybrid. *Journal of Forest Research*, short communication, 21:4, pp. 514-516.
- Munalula, F., Meincken, M. (2009). An evaluation of South African fuel wood with regards to calorific value and environmental impact. *Journal Biomass and Bioenergy*, 33, pp. 415-420.
- Parr. (1999). 1266 Isoperibol Bomb Calorimeter. Operating Instruction Manual. Technical Note No. 367M. Parr Instrument Company. Illinois, USA.
- PNUD, GEF, CONAFOR, RAINFOREST. (2014). Biodiversidad en Bosques de Producción y Mercados Certificados Catálogo de maderas tropicales de México. 10/10/2017, de Programa de las naciones unidas para el desarrollo.
- Ramírez-Guardado, M. A. 2015. Estimación del carbono retenido en la biomasa aérea, en una selva tropical de Yucatán, México. Tesis de maestría en Energía Renovable. Centro de Investigación Científica de Yucatán, AC, México, p.111.
- Tancredi, N., Amaya, A., Medero, N. (2005). Residuos de Madera de Bosque Tropical: Obtención de Carbón Activado y Determinación de Poder Calorífico, Montevideo Uruguay), Congreso Interamericano de Residuos. Mérida.
- Technical Association of the Pulp and Paper Industry (TAPPI). (2006). Preparation of wood for chemical analysis. T 257 cm-85. TAPPI Test Methods. Fibrous Materials and Pulp Testing. Atlanta, GA., U.S.A.

Telmo, C., Lousada, J. (2011). Heating values of wood pellets from different species, *Journal Biomass and Bioenergy*, 35, pp. 2634-2639.

Vassilev, S. V., Baxter, D., Andersen, L. K., Vassileva, C. G. (2010). An overview of the chemical composition of biomass. *Fuel*, 89:5, pp. 913-933.

The ferrite nanoparticles (Fe_2O_3) impact on germination, growth and lignine content of carrot (*Daucus carota*)

VAZQUEZ-NUÑEZ, Edgar^{1*}†, VALLE-GARCIA, Jessica Denisse¹, and CASTELLANO-TORRES, Laura Edith¹

Universidad de Guanajuato. División de Ciencias e Ingenierías. Campus León. Departamento de Ingenierías Química, Electrónica y Biomédica, Lomas del Bosque 103 Col. Lomas del Campestre. León, Guanajuato, México, C.P. 37150. Tel. (477) 7885100 Ext. 8493

Received July 18, 2017; Accepted November 25, 2017

Abstract

This study investigated the effect of ferrite (Fe_2O_3) Nanoparticles (NPs) on carrot plantlets (*Daucus carota*). Seeds were soaked during twelve hours in NPs solutions at 50, 500 and 1000 mg L⁻¹ (T1, T2, T3), and a control treatment (TC) during 14 days. It was measured the root length and germination percentage at 3, 7 and 14 days; Kotowski's coefficient was estimated at 14 days. Raman spectroscopy was used to analyze samples TC, T1 and T3 at 7 days of germination. Results showed an effect of NPs on plantlets. Inhibition of germination measured as germination percentage was found with NPs, but the growth rate was higher at 500 mg L⁻¹. There was an inhibition of total seeds treated with solution at 1000 mg L⁻¹ but the maximum value of root length was obtained in seeds soaked at 50 mg L⁻¹. Finally, in Raman spectroscopy it was observed a positive relationship between NPs concentration and lignin content in plant tissue; this represent a possible modification on the composition and concentration after to addition of NPs on wall cell of plant.

Vegetable, Raman spectroscopy, Kotowski's coefficient

Citation: VAZQUEZ-NUÑEZ, Edgar, VALLE-GARCIA, Jessica Denisse, and CASTELLANO-TORRES, Laura Edith. The ferrite nanoparticles (Fe_2O_3) impact on germination, growth and lignine content of carrot (*Daucus carota*). ECORFAN Journal-Ecuador. 2017, 4-7:8-14

*Correspondence to Autor (E-mail: edgar.vazquez@ugto.mx)

† Researcher contributing as first author.

Introduction

Nowadays nanotechnology has opened doors in the different fields worldwide, e.g., agriculture, biotechnology, industries, medicine, because it is common to use Nanoparticles (NPs) that have unique characteristics, and physical and chemical properties with millions of applications (Siddiqui, 2015). This NPs can interact with plants causing morphological and physiological changes (Siddiqui, 2015). NPs interact with roots and shoots; size and surface properties of NPs can influence the pathways (Dietz and Herth, 2011). Another way is for xylem; xylem diameter determines the size of the particle that can be transported and also the speed of water transport (Ma *et al.*, 2010).

Ma *et al.*, 2010, and other suggested that these nanomaterials have both positive and negative effects on plant growth and depends on the composition, concentration, size, and physical and chemical properties of NPs as well as plant species. The unique properties of NPs could affect crop plants or stimulate the food and agriculture production. Some examples of this nanomaterials are the metal based nanomaterials: Fe, Cu, Zn, Ti, etc (Zurvez-Mena *et al.*, 2016).

E. g. the utilization of iron based nanomaterials is being widely studied. The use of this NPs is many common because it is simple and the synthesis has a low cost so it makes them available from the industrial producers (Deliyanni *et al.*, 2004; Waychunas *et al.*, 2005; Mohapatra and Anand, 2010; Mueller *et al.*, 2012). The main use of this NPs is about remediation purposes from contaminated waters and soils (Gómez-Pastora *et al.*, 2014), because the iron oxide NPs can also be easily separated and recovered due their magnetic properties (Gómez-Pastora *et al.*, 2014).

According to different experiments this NPs are considered non-toxic to the environment because are poorly absorb by organism (Zhu *et al.*, 2008) but their potential adherence to the root surface cause adverse effects in plants when administered in relatively high concentrations (Zuverzá-Mena *et al.*, 2016).

Material and methods

Seed conditioning

Carrot seeds were stored at 25 °C, after the seeds were washed with a solution of sodium hypochlorite 0.6% and washed out three times with distilled water.

Nanoparticles

Ferrite NPs (~ 30 nm) were selected to carried out the study. NPs acquired from the laboratory Materiales nanoestructurados S.A. de C.V.

Treatments

We established four treatments: a) treatment control (TC), distilled water without Fe₂O₃ nanoparticles; b) treatment T1: Solution of NPs-Fe₂O₃ at 50 mg L⁻¹; c) treatment T2: NPs-Fe₂O₃ solution at 500 mg L⁻¹; d) treatment T3: NPs-Fe₂O₃ solution at 1000 mg L⁻¹.

Incubation in Petri dishes

The washed seeds were placed into the nanoparticles solutions during six hours and put in petri dishes. Each treatment was carried out per triplicate. The petri dishes were incubated at 28±5°C during 14 days. The total number of experimental units was 15.

Sampling and measurements

The samples were taken at 3, 7, 14 days. It was calculated the germination percentage and the germination rate coefficient (Kotowski coefficient); the root length was measured.

VAZQUEZ-NUÑEZ, Edgar, VALLE-GARCIA, Jessica Denisse, and CASTELLANO-TORRES, Laura Edith. The ferrite nanoparticles(Fe₂O₃) impact on germination, growth and lignine content of carrot (*Daucus carota*). ECORFAN Journal-Ecuador.2017.

The Raman spectroscopy was used in order to determine the effect of the NPs on the surface of plant.

Statistical analysis

The data obtained were analysed by using the statistical software XLStat®. For the germination rate and Kotowski's coefficient ANOVA were performed assuming 95% of confidence range and tolerance of 0.0001; the graphics of standardized coefficient were used to probe statistical differences. For the analysis of the length root measurements a Principal Component Analysis (PCA) was performed taking the factors with most impact on the behaviour of the active observations. The plots of variables and factors, factors and observations was showed and clusters were built. The PCA analysis was performed considering 5% of significance.

Results

Kotowski's coefficient and germination percentage

The germination percentage was measured at 3, 7 and 14 days of incubation in petri dishes. Table 1 shows the results for this variable in which there is a significant difference between the number of seeds germinated at control treatment TC (1000 mg L⁻¹) i.e, 94% at 14 days compared with treatment T3, i.e, 38%. A positive correlation is observed between the germination rate and the NPs concentration.

On the other hand, the growth velocity coefficient was estimated at 14 days. Table 2 shows that even with NPs the Kotowski coefficient is higher in T2 compared with others. TC and T3 obtained the same result.

Concentration (mg L ⁻¹)	Germination percentage		
	Day 3	Day 7	Day 14
TC	25.0±2 ^a	76.0±10 ^a	94.0±3.5 ^a
T1	0.00±0 ^b	89.0±5.1 ^a	85.0±8.4 ^a
T2	46.0±9 ^c	50.0±9.1 ^b	46.0±4.7 ^b
T3	0.00±0 ^b	33.0±5.3 ^c	38.0±5.2 ^b

n = 9, 3 experimental units per triplicate
Same capital letters are not statistically different among treatments by the Tukey test (p < 0.001).

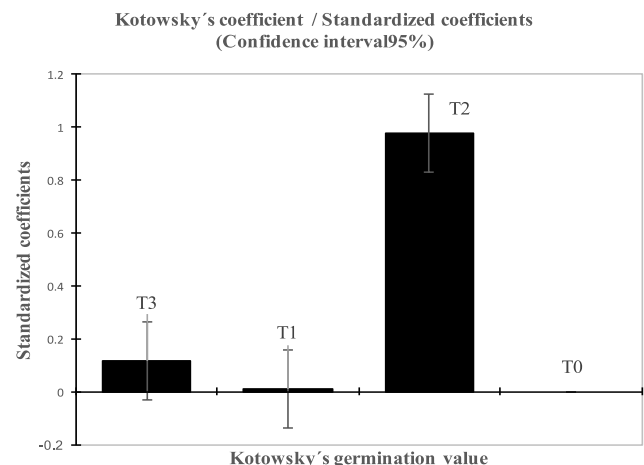
Table 1 Germination percentage at 3, 7 and 14 days of treatment

Concentration (ppm)	Kotowski's coefficient at 14 days
TC	9.90
T1	9.00
T2	14.1
T3	9.90

Table 2 Kotowski coefficient calculated at 14 days of germination

The above data were statistically analyzed by applying ANOVA analysis (XLStat®), confidence 95% and tolerance 0.001.

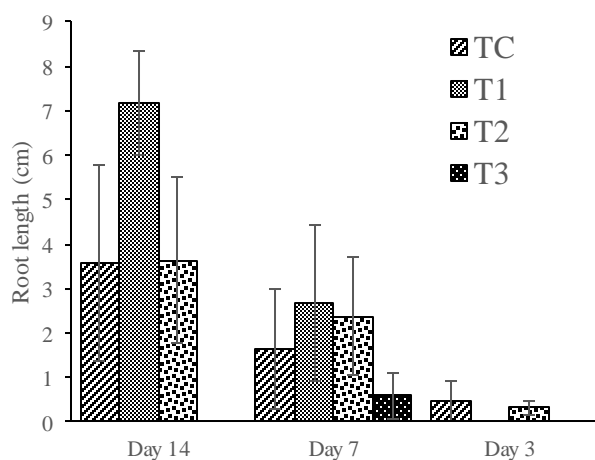
The graphic 1 shows the standardized coefficient's and confirm the statistical difference between treatments.



Graphic 1 Mean value and standard deviation for the Kotowsky's coefficient observed in the three treatments

Root length

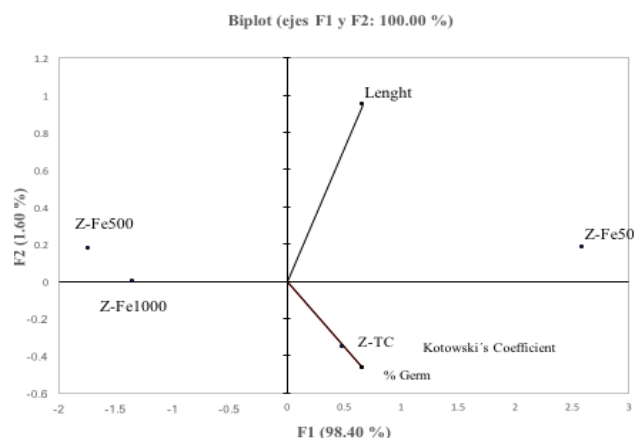
About the root length at 3 days we only could measure TC and T2. It took 7 days to observe a significant root length in four treatments. However, it was treatment T1 (50 mg L⁻¹) which reached the greatest length. At day 14th the seeds in T2 grew 7 cm; this was significant compared with control.



Graphic 2 Root length for the four treatments at 3, 7 and 14 days of germination

Principal Component Analysis

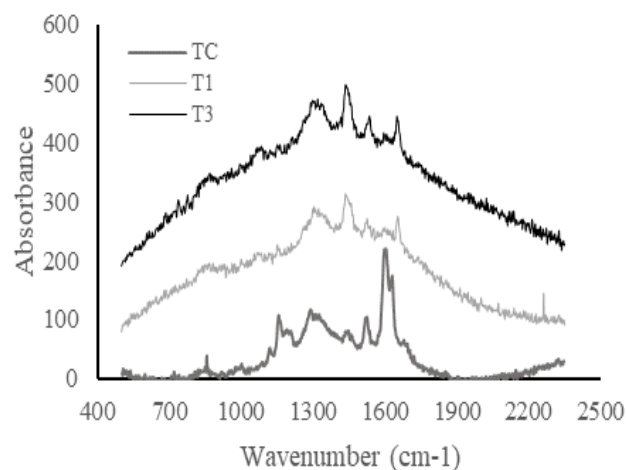
A Principal Component Analysis (PCA) was carried out for all the variables at day 14, in order to determine the percentage of explanation for variables involved in the experiment. The figure X. shows the behaviour of the variables i.e., root length, Kotowsky's coefficient and percentage of germination (%).



Graphic 3 Principal Component Analysis for the most important variables after 14 days of experimental set up

Raman spectroscopy

It was found an effect of NPs on cell wall of plant according to the spectrum of Raman. Graphic 4 shows the differences between the peaks obtained to TC and T1, T3. At 1600 cm⁻¹ exists a decrease in the intensity of peaks for T1 and T3. And the shape of the spectrum changes relatively.



Graphic 4 Raman spectroscopy for carrot at 7 days for treatments TC, T1, and T3

Discussion

Many of studies provide evidence that plant uptake is a potential transport pathway of NPs in the environment (Zhu *et al.*, 2008). Libralato *et al.*, 2016, observed that germination depends on Fe form and plant species; they observed biostimulation effects on seedling length and biomass production using zero valent iron on germination in *Lepidium sativum* and *Sorghum saccharatum* in petri dishes. Wang *et al.*, 2016 found damages in root tissue and chlorophyll reduction with Fe NPs.

In this study, there was a statistical difference on the germination seeds percentage, we found that seeds treated with NPs had a low percentage compared with control treatment. However, the seeds soaked in 500 mg L⁻¹ showed the maximum values for Kotowski's coefficient (14.1) compared with TC (9.90); TC and T3 had the same value.

It was our interest analyze the effect of the interaction of other variables in the final value; a PCA was performed and it was observed that there was an effect of the Fe-NPs at 50 mgL⁻¹ and it was related with the length of the plantlets in a positive form, contrarely, the treatments ant 500 and 1000 mgL⁻¹ did not have any relation with the variable analyzed. The seeds under zero Fe-NPs treatments showed the maximum values for germination percentage and Kotowski's coefficient after 14 days of experimentation, as is observed in Figure 3.

According to morphological analysis we found differences between treatments; analyzing the root length it was found that treatment T1 had the maximum value at 14 days of incubation while root length of T3 was reduced even we can assume that at this NPs concentration plants die.

Reported results of experiment carried out with Fe NPs at different concentrations i.e, nFe₂O₃ at 0.25, 0.5, 0.75 and 1 g L⁻¹ have obtained the follow data: in soybean the NPs increased leaf and pod dry weight; nFe₃O₄ at 0.67 mg mL⁻¹ during 7 days it was found a total inhibition of germination in lettuce, radish, cucumber, spinach, tomato and peppers and at 0.5 g L⁻¹ in less of 20 days in pumpkin plants its reported a translocation through out the plant tissues, NPs detected in stem and leaves and accumulation on the root surface (Sheykhbaglou *et al.*, 2010; García *et al.*, 2011; Zhu *et al.*, 2008).

Our research group found that were not statistical differences on length root and germination percentage in alfalfa (*Medicago sativa*) and broccoli (*Brassica oleracea italica*) plantlets after soaking in Fe nanoparticle at different concentrations (50 mg L⁻¹, 500 mg L⁻¹ and 1000 mg L⁻¹) (Data no published).

Same results were obtained when carrot seeds were soaked in Ti-NPs and the length root was measured after 14 days of incubation, the enhanced effect on root length of Ti-NPs was observed in alfalfa seeds after 14 days of incubation (Data no published).

On the other hand, the Raman spectroscopy results showed a positive relationship between NPs concentration and the lignine content in the plants tissue. It is possible to observe a representative peak at 1600 cm⁻¹; Gierlinger *et al.*, 2007 reported the same results in plants tissues analysis at this wavenumber; it is associated with the lignin phenyl ring, which is the main component of the wall cell of plants; these results allow us to suppose that the plant tissues might have modification in the lignin composition and concentration after addition of NPs.

Conclusions

The results obtained in this study show that metal oxide nanoparticles like iron NPs might have a potential effect on carrot seeds; we found that at moderate concentration the growth rate may be enhanced but the germination percentage and the root length at elevated concentration of NPs could be inhibited, however seeds treated with a small amount of NPs (50 mg L⁻¹) had a significant difference in root length at 14 days; this treatment had the higher root length. A reduction of the lignine amount in plant tissue was detected via spectroscopy analysis using Raman technique.

Acknowledgements

The authors would like to thank the financial support to Prodep Project PTC UGTO-PTC-57 and to the University of Guanajuato for the facilities.

References

- Deliyanni, E.A., Lazaridis, N.K., Peleka, E.N., Matis, K.A. (2004) Metals removal from aqueous solution by iron-based bonding agents. *Environ. Sci. Pollut. Res.* 11, 18-21.
- Dietz, K.J., Herth, S., (2011) Plant nanotoxicology. *Trends Plant Sci.* 16, 582-589. European Union, Commission Delegated Regulation No. 1363/2013 of 12 december 2013. Official Journal of the European Union, L 343/26-L343/28.
- García, A., Espinosa, R., Delgado, L., Casals, E., Gonzalez, E., Puentes, V., Carlos, B., Font, X., Sanchez, A., (2011) Acute toxicity of cerium oxide, titanium oxide and iron oxide nanoparticles using standardized tests. *Desalination* 269, 136-141.
- Gierlinger, N., Schwanninger, M. (2007) The potential of Raman microscopy and Raman imaging in plant research. *Spectroscopy* 21, 69-89.
- Gómez-Pastora, J., Bringas, E., Ortiz, I. (2014) Recent progress and future challenges on the use of high performance magnetic nano adsorbents in environmental applications. *Chem. Eng. J.* 256, 187-204.
- Libralato, G., Costa Devoti, A., Zanella, M., Sabbioni, E., Micetic, I., Manodori, L., Pigozzo, A., Manenti, S., Groppi, F., Volpi, G.A., (2016) Phytotoxicity of ionic, micro- and nano-sized iron in three plant species. *Ecotoxicol. Environ. Safe* 123, 81-88.
- Ma X, Geiser-Lee J, Deng Y, Kolmakov A (2010) Interactions between engineered nanoparticles (ENPs) and plants: phytotoxicity, uptake and accumulation. *Sci Total Environ* 408(16):3053–3061.
- Mohapatra, M., Anand, S. (2010) Synthesis and applications of nano-structured iron oxides/hydroxides e a review. *Int. J. Eng. Sci. Technol.* 2 (8), 127-146.
- Mueller, N.C., Braun, J., Bruns, J., Cerník, M., Rissing, P., Rickerby, D., Nowack, B. (2012) Application of nanoscale zero valent iron (nZVI) for groundwater remediation in Europe. *Environ. Sci. Pollut. Res.* 19, 550-558.
- Sheykhbaglou, R., Sedghi, M., Tajbakhsh Shishevan, M., Seyed Sharifi, R. (2010) Effects of nano-iron oxide particles on agronomic traits of soybean. *Not. Sci. Biol.* 2, 112-113.
- Siddiqui M, Al-Whaibi M, Firoz M, Al-Khaishany Y (2015) Role of nanoparticles in plants. Siddiqui, Manzer H, Al-Whaibi, Mohamed H, Mohammad, Firoz. *Nanotechnology and plant sciences.* (pp. 19-21).
- Wang, J., Fang, Z., Cheng, W., Yan, X., Tsang, P.E., Zhao, D., (2016) Higher concentrations of nanoscale zero-valent iron (nZVI) in soil induced rice chlorosis due to inhibited active iron transportation. *Environ. Pollut.* 210, 338-345.

Waychunas, G.A., Kim, C.S., Banfield, J.F. (2005) Nanoparticulate iron oxide minerals in soils and sediments: unique properties and contaminant scavenging mechanisms. *J. Nanopart. Res.* 7, 409-433.

Zhu, H., Han, J., Xiao, J.Q., Jin, Y. (2008) Uptake, translocation, and accumulation of manufactured iron oxide nanoparticles by pumpkin plants. *J. Environ. Monit.* 10, 714-717.

Zuverza-Mena, N., Martínez-Fernández, D., Du, W., Hernandez-Viezas, J., Bonilla-Bird, N., Lopez-Moreno, M., Komárek, M., Peralta-Videa, J., Gardea-Torresday, J. (2016) Exposure of engineered nanomaterials to plants: Insights into the physiological and biochemical responses-A review. *Plant Physiology and Biochemistry*, 1-29.

Synthesis and characterization of Pd/TiO₂ thin films with possible applications in photocatalysis

TIRADO-GUERRA, Salvador*† and VALENZUELA-ZAPATA, Miguel

Received July 18, 2017; Accepted November 25, 2017

Abstract

Synthesize thin Pd/TiO₂ films on soda-lime glass substrates, using the sol-gel chemical route and repeated immersion. Salt at 0.2 M Ti (IV) oxy acetylacetonate is dissolved in 2-methoxyethanol and stabilized with monoethanolamine, solution that is aged to obtain TiO₂ films sintered at 250 °C in air and thermal treated at 400 °C. They are surface modified with layers of palladium from a solution, following the procedure and thus the Pd/TiO₂ films. The physical and chemical properties of the prepared films are studied. The Pd/TiO₂ films are characterized in structure (XRD), morphology (SEM), chemical composition by EDS, topography (AFM), optical properties (UV-Vis) and surface analysis by XPS. Film thicknesses of 172.8 nm, a crystallite size of the order of 20 nm, transmittance of 85%, refractive indexes between 2.046-1.599, a semiconductor bandwidth of 3.67-3.50 eV, depending on the layers of palladium, resulted. The photocatalytic properties thereof were recorded, when evaluating the degradation of an aqueous test solution, as a function of the concentration and time of UV-A irradiation. The photoluminescent properties of the films were evaluated when excited with 325 nm photons. They could be applied in the treatment of water, and in radiation dosimetry.

TiO₂, sol-gel, Thin Film, Photocatalysis, Photoluminescence, Palladium

Citation: TIRADO-GUERRA, Salvador and VALENZUELA-ZAPATA, Miguel. Synthesis and characterization of Pd/TiO₂ thin films with possible applications in photocatalysis. ECORFAN Journal-Ecuador. 2017, 4-7:15-25

*Correspondence to Autor (E-mail: tirado@esfm.ipn.mx)

† Researcher contributing as first author.

Introduction

Air pollution and wastewater produced in the textile industry or in the field where technically sophisticated fertilizers, pesticides and/or detergents are used, it is quite a problem to be solved. The degradation of polluting compounds can be achieved with reactions where redox processes occur. Solar radiation can cause reactions in wide variety of organic compounds but in a limited way, as high energy (>3.3 eV) are required. Photosynthesis is a phenomenon that can remove harmful organic compounds using photo-catalysts as oxides such as TiO_2 , ZnO or SnO_2 , which are also used in catalysis (Malagutti, A.R., et al., (2009), Nejand, B.A., et al., (2010), Xin, B., et al., (2008)).

They can be simple or complex as TiO_2/WO_3 which was used to degrade rhodamine B or methyl orange (Ge, M., et al., (2009)), or composites such as ZnO/TiO_2 (Liu, G., et al., (2009)a, Ge, M., et al., (2009)) and $\text{Cu}_2\text{O}/\text{T-ZnOw}$ (Liu, G., et al., (2009)b). The degrading efficiency of a catalyst is tested with a tracer substance, based on the evaluation of the degree of degradation and mineralization to H_2O or a clean or treatable product, which is usually carried out with UV-Vis spectroscopy (Hou, J.R., et al., (2007), Ge, M., et al., (2009)).

A semiconductor such as TiO_2 or similar systems can be excited with UV radiation and from the absorbed photons, charge carriers are generated as e^- and h^+ , where the electron is ejected from the valence band VB leaving a hole, and transferred to the conduction band CB, generating electron-hole pairs (Nejand, B.A., et al., (2010)). The pairs produced can participate in reactions that decompose contaminating molecules found in the environment. Catalytic semiconductor response to UV irradiation depends on various factors: the catalyst structure, radiation, the preparation method, etc. (Xin, B., et al., (2008), Nejand, B.A., et al., (2010), Malagutti, A.R., et al., (2009)).

The photocatalytic efficiency of the semiconductor thin films (TiO_2 , ZnO) commonly improved by doping with metallic or non-metallic ions (Xin, B., et al., (2008), Chen, H., et al., (2016)) and/or deposit of precious metals (Cu, Ag, Pd), which generate levels-energy between the VB and CB bands, as vacancies, among others, which improve the optical and electrical properties, as well as photocatalytic and photoluminescence (Chae, Y.K., et al., (2013), Liu, H., et al., (2013), Dinh, C.T., et al., (2011), Malagutti, A.R., et al., (2009), Li, Q., et al., (2009), Liu, B., et al., (2014), Liu, J., et al., (2016), Wang, F., et al., (2015)).

Preparing of thin $\text{Ag}:\text{TiO}_2$ films by the polymeric precursor method, Malagutti, et al. (Malagutti, A.R., et al., (2009)) makes applications in photodegradation of textile dyes, while Dinh et al. (Dinh, C.T., et al., (2011)) using photodeposition growing techniques, colloidal clusters of Ag on TiO_2 nanocrystals which are applied in photodegradation of methylene blue and rhodamine B (Liu, F., et al., (2016)).

In this work, the synthesis of semiconductors in Pd/TiO_2 thin film prepared by the sol-gel chemical route (Brinker C.J. (1990)) and the dip coating method, as well as the study, are described. For this purpose, a series of TiO_2 films of the same thickness and then the series of Pd/TiO_2 surface modified films were prepared with several palladium deposits, the films were sintered in air at 250°C and thermally treated at 400°C . Thin films were characterized by XRD, EDS, surface properties by SEM and AFM, and their optical properties by UV-Vis. The Ti, O and Pd ionization states were determined by XPS, which is reported in the study. The effect of both, palladium deposits and conditions of preparation, on the photocatalytic properties of the films in the degradation of an aqueous solution of methyl orange (MO) at 14 ppm, and also which are the effects on their emission spectra, when samples are irradiated with UV (325 nm), evaluated.

From such study, determine the possible of application of Pd/TiO₂ films, in homogeneous photocatalysis and in radiation dosimetry, to mention this two cases. Since the thin-film TiO₂ semiconductor has a bandwidth of the order of 3.2 eV, it is known that it can be modified, in fact reduced, when the film is doped with metals of Au, Ag, Cu, among others, or is superficially modified with similar materials, such as Pd. Thus, using the method of the chemical route and repeated immersion, technique already implemented, Pd/TiO₂ films from appropriate precursors will be synthesized, varying the palladium deposits and at a temperature of 250 °C and a thermal treatment at 400 °C.

It is desired to study the effect on the structural, morphological and optical properties of the films, as well as the photocatalytic properties when irradiating with UV-Vis and degrading a tracer substance, and the photoluminescence presented by the Pd/TiO₂ series of films when they are irradiated with UV.

The order of presentation is, introduction and justification, methodology experimental, synthesis, characterization techniques, results and discussion are given by technique: XRD, SEM and EDS, AFM, UV-Vis and XPS, photodegradation and photoluminescence, conclusions, acknowledgments and references.

Methodology experimental

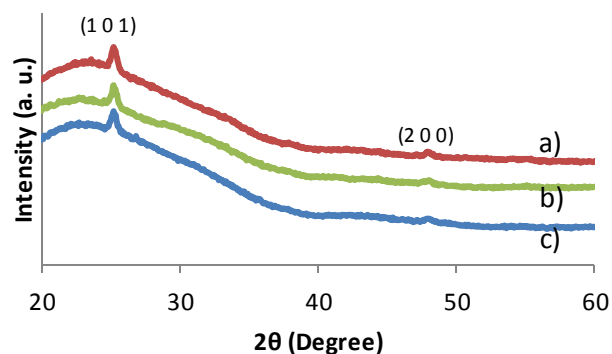
Synthesis

Series of Pd/TiO₂ films were prepared by the sol-gel route, and dip coating technique, from a solution (100 mL) of titanium oxy-acetylacetonate (IV) salt (TiO(C₅H₇O₂)₂) at 0.2 M in 2-methoxyethanol (C₃H₈O₂) as solvent, and monoethanolamine ((C₂H₅O)NH₂) as stabilizer at 23 °C, for 2 h with constant magnetic stirring, and an aqueous solution of palladium nitrate dihydrate (N₂O₆Pd•2H₂O) at low concentration. The solution was aged for seven days before being used in the growth of films. The samples resulted with an average thickness of 172.8 nm.

X-ray diffraction

Diffraction patterns were recorded on a PANalytical X'Pert PRO MRD diffractometer model, with Cu tube K_α (λ = 0.15406 nm) at 45 kV voltage and 40 mA of tube current, using the Bragg-Brentano geometry, θ-2θ, the spectra were recorded in the range of 15-80° with a step of 0.03° and time of 200 s accounts with an aperture of 0.5°. XRD diffractograms of the Pd/TiO₂ films were polycrystalline with diffraction peaks at 25.281, 36.947 and 48.050° to name a few, and they correspond to the (1 0 1), (1 0 3) and (2 0 0) planes, respectively (see graphic 1).

These drawings were indexed according to 021-1272 card of TiO₂ anatase phase (tetragonal, space group 141/amd with cell parameters: a = b = 3.7852 Å and c = 9.5139 Å at 90° angles, the known Scherrer's formula, $D = 0.9 \lambda / \beta \cos \theta$, with λ wavelength of Cu K_α (λ = 0.15406 nm), θ is angular peak position and β is the semi-width of the peak given in radians, was used to estimate the crystallite size, and resulted a D ~ 20 nm.



Graphic 1 Diffraction patterns of Pd/TiO₂ films, (a) for pure sample, (b) with one layer of palladium and (c) samples with three layers of palladium.

Scanning electron microscopy

SEM micrographs of Pd/TiO₂ films were recorded on a QUANTA 3D FEG SEM microscope (FEI) and representative x10000 magnification micrographs are shown in Fig. 2a) and 2b).

The micrograph of the Pd/TiO₂ pure films (Fig. 1a)) has an uneven and porous morphology, however for micrograph in Fig. 1b) of the Pd/TiO₂ films with a surface deposited with Pd can be observed a morphology more uniform with fine grains and growth in areas (lights) corresponding to nanoparticles of Pd, with EDS analysis the presence of palladium nanoparticles was detected, the surface distribution of the growth of the nanoparticles was uniform, making more evident the surface distribution and increased grain size (image not shown).

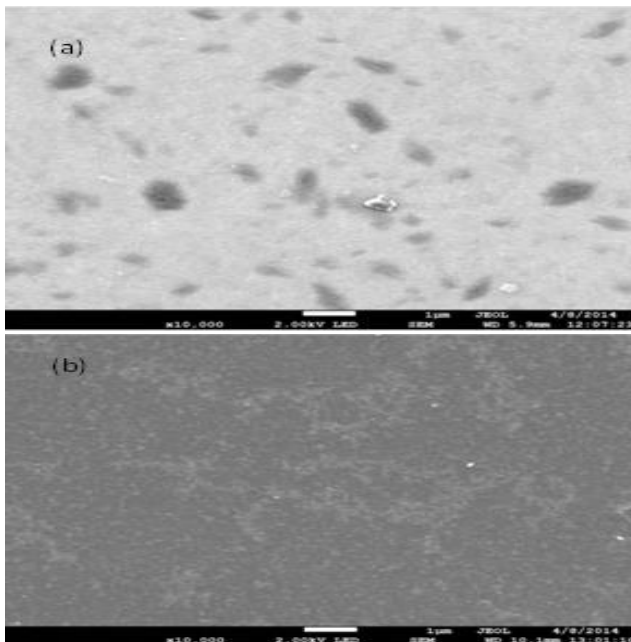


Figure 1a) and 1b) SEM micrographs increased x10000, (a) Pd/TiO₂ pure and (b) Pd/TiO₂ samples with one layer of palladium

Atomic force microscopy

Topographical and morphological characteristics of Pd/TiO₂ films were recorded on a Park AutoProbe CP Equipment, atomic force microscope (Veeco) with a tip of silicon 10 microns, intermittently. 3D topographical (AFM) representative images of Pd/TiO₂ pure and modified films with a layer of palladium are shown in Fig. 2a) and 2b), respectively. It is observed the grain surface density in the order of 42 grains/µm².

In the 2D image of Fig. 3, the marker line and the corresponding profile, the distribution and grain sizes are shown. The average grain size is really small (around 0.1 µm or less) and roughness parameters were, Rq = 1.16 nm and Ra = 0.886 nm in a 1x1 µm².

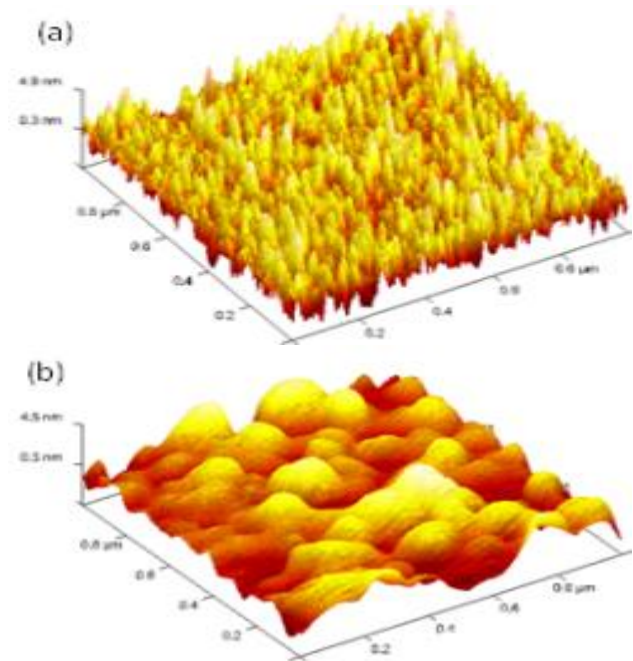


Figure 2a) and 2b) 3D images AFM, (a) Pd/TiO₂ pure and (b) Pd/TiO₂ with one palladium layer, respectively

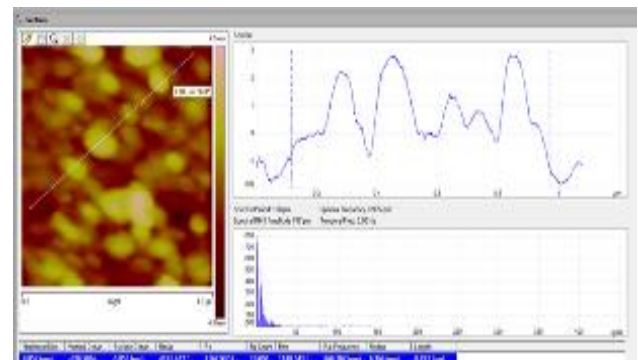
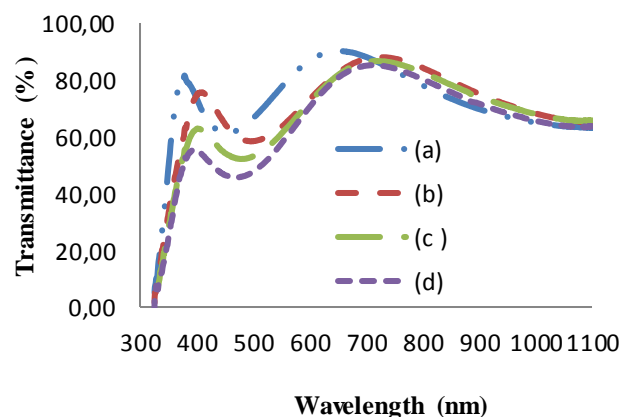


Figure 3 2D image of Pd/TiO₂ with a palladium layer and the cross-sectional profile indicated in the picture

Ultraviolet-visible spectroscopy

UV-Vis spectra of Pd/TiO₂ films (graphic. 2) were recorded on a UV-Vis Perkin Elmer model Lambda 2 spectrophotometer, a deuterium lamp (²H) was used for the UV region and a tungsten one for the visible region, the spectra were recorded in the range of 190-1100 nm in wavelength. The board absorption was recorded in 381 nm (pure) and at 417 nm for the film with a layer of Pd, while the transmittance was 85 % and 80 %, respectively. From the visible part of spectra the thickness of the films was estimated at 172.8 nm in pure films and 162.4 nm in films with a layer of Pd.

The indices of refraction were in the range of 2.046-1.599 and 2.262-1.672 for pure sample and for samples with a layer of Pd, respectively, the refractive index of samples with more catalyst deposits were in the order. Likewise, in the region of high energies of these spectra the bandwidth E_g of Pd/TiO₂ semiconductors, was evaluated, resulting 3.67, 3.62 and 3.50 eV for pure sample, and with 1 and 3 layers of palladium, respectively, it can be observed a red shift when the layers of Pd are increased, and using the fact that the TiO₂ semiconductor has an indirect band, from a graph of $(kh\nu)^{1/2} = A(h\nu - E_g)$ extrapolation to the axis of photons. A is a constant and k is related to the Kubelka-Munk constant, the E_g value was obtained (Murphy, A.B., et al., (2007), Patcharee, J., et al., (2012), Ilican, S., et al., (2008)). The relationship $\alpha(\lambda) = \ln(1/T)/d$ gives the dependence of the refractive index with wavelength λ , was used to obtain the value for d film thickness.



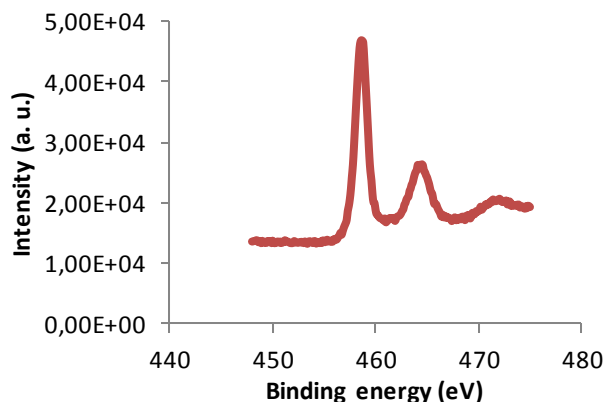
Graphic 2 UV-Vis spectra of the Pd/TiO₂ films, (a) pure film, and (b), (c) and (d) films with one, three and five layers of palladium

Spectroscopy of photoelectron

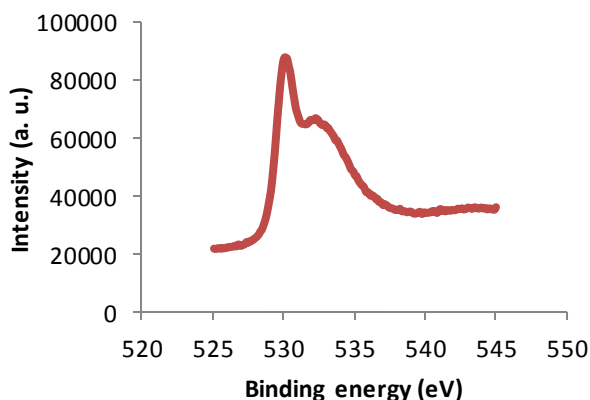
Through spectroscopy of photoelectron (XPS) (Thermo Scientific K Alfa, Double Source Mg and Al) the ionization states of Ti, O, and Pd, and the binding energies of the respective orbitals, were evaluated. Graphic 3 shows the high resolution XPS spectra for the Ti2p (graphic 3) orbital, O1s (graphic 4) orbital, and the Pd3d orbital (graphic 4), respectively. The energy of the Ti2p (2p_{3/2}, 2p_{1/2}) orbital, with maximum intensities at 458.78 and 464.58 eV, respectively, for systems of TiO₂:Cu prepared by sol-gel, Xin et al. evaluated the energy of the 2p_{3/2} level at 458.1 eV (Xin, B., et al., (2008)). For O1s, the highs in 530.28 and 533.88 eV linked to species of oxygen, e.g. oxygen of lattice and possible oxygen adsorbed, respectively (Dinh, C.T., et al., (2011), Liu, H., et al., (2013), Liu, F., et al., (2016)).

From the spectra recorded for the Pd/TiO₂ systems, the orbital energy of Pd3d (3d_{5/2}, 3d_{3/2}), the maximum values resulted around 336.88 and 342.28 eV, respectively, Brun, M., et al. reported for the 3d_{5/2} orbital, 335.4 eV (Brun, B., et al., (1999)). It is observed a sub-structure in the high resolution spectrum Pd3d (335.48 and 340.98 eV) with a $\Delta E = 5.50$ eV.

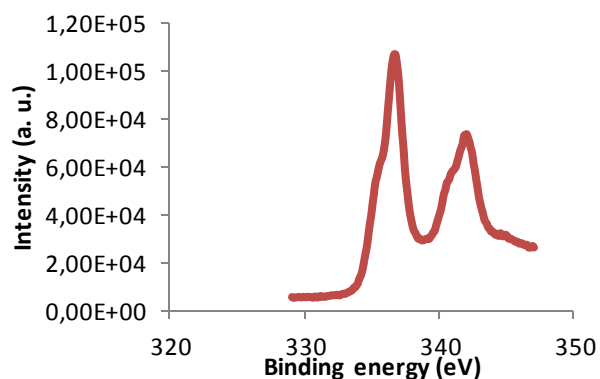
The Pd3d double peaks can show the presence of metallic Pd and PdO as reported (Hoflund, G.B., et al., (2003), Brun, B., et al., (1999)). All peaks of spectra were determined relative to the energy of the carbon C1s orbital (284.68 eV), that gives the calibration for the peaks in the spectra of Pd/TiO₂ semiconductors.



Graphic 3 High resolution XPS spectrum of the orbital Ti2p (2p_{3/2}, 2p_{1/2}) at 458.78 and 464.58 eV in binding energy, respectively.



Graphic 4 High resolution XPS spectrum of the O1s orbital with peaks at 530.28 and 533.88 eV in binding energy that can be linked to different oxygen species.



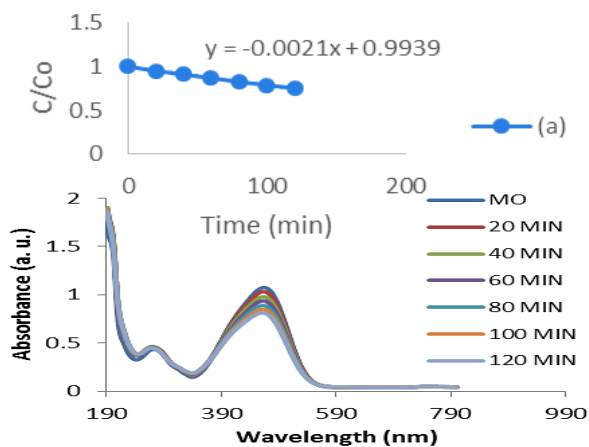
Graphic 5 Energy of Pd3d orbital (3d_{5/2}, 3d_{3/2}), the maximum values resulted around 336.88 and 342.28 eV, respectively. The Pd3d double peaks can be observed.

Photocatalytic activity

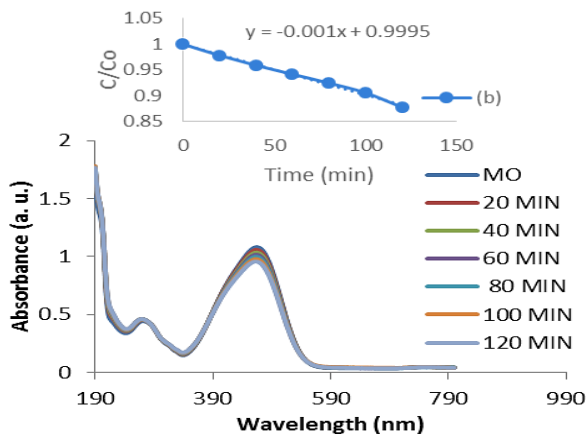
The photocatalytic properties of the Pd/TiO₂ catalysts were probed in the degradation of an aqueous solution of methyl orange to 14 ppm, irradiating the samples of 1 cm² area (two-sided) with six fluorescent lamps at different times in a photo-reactor Luzchem LCZ-5 and the photo-degradation of the solution in the 190-800 nm range, was registered in a Cintra 20 of GBC spectrophotometer, while from an integrating sphere the diffuse absorbance of the solution was evaluated, 100 mL of aqueous solution of methyl orange were prepared in volumetric flask, from which were used aliquot of 3 mL.

The procedure was to record the absorbance of the non-irradiated aliquot and from the main band at 464.0 nm, its evolution was followed when the aliquot-catalyst system, was irradiated each 10 min until completing 120 min. The behavior of a set of 4 samples (pure, and those with 1, 3 and 5 deposits of palladium) was recorded. If C₀ is the initial concentration and C the concentration of the solution for a given irradiation time, the kinetics of the reaction follows the equation $K[C] = -d[C]/dt$, and when it is integrated gives $\ln[C]/[C_0] = -k^t$, and the plot of $\ln[C]/[C_0]$ versus irradiation time, t , the slope corresponds to the pseudo reaction constant (Malagutti, A.R., et al., (2009), Liu, F., et al., (2016), Wang, F., et al., (2015)).

In order to show the catalytic activity of Pd/TiO₂ semiconductors, it is given in graphic 6 and graphic 7, the TiO₂ catalytic response of the pure systems and films with one palladium layer, spectra correspond to the non-irradiated aqueous solution and for 20, 40, 60, 80, 100 and 120 min irradiation time (each case). The insert slope in graphs shown, are related to the constant of the reaction. It is expected that systems with several palladium deposits present a greater catalytic activity than those corresponding to the pure TiO₂ system.



Graphic 6 Photodegradation of the pure TiO₂ film depending on the wavelength, and the inserted graph showing the variation of the concentration of the solution as a function of irradiation time.

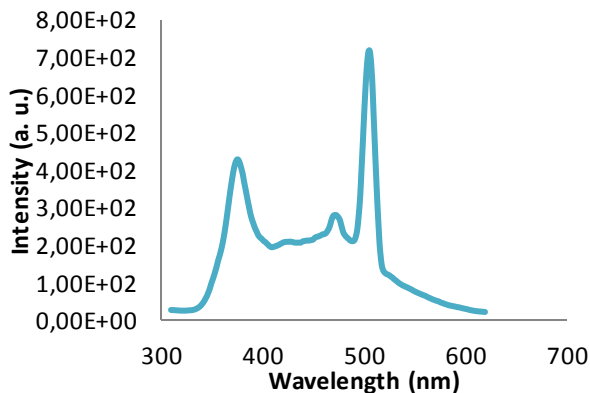


Graphic 7 Photodegradation of Pd/TiO₂ film with one palladium layer, depending on the wavelength, and the inserted graph showing the variation of the concentration of the solution as a function of irradiation time.

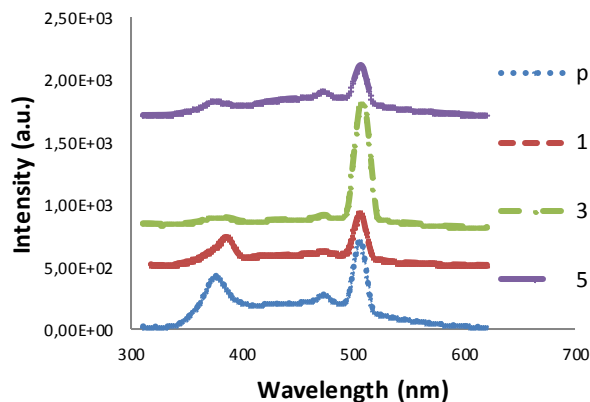
Photoluminescence

The luminescent properties of the Pd/TiO₂ films were recorded at room temperature in a Shimadzu RF-5301 spectrofluorophotometer. The excitation energy corresponds to a wavelength of 325 nm, and the corresponding emission spectra were recorded in the 310 to 620 nm range. Three major bands are defined in the photoluminescence spectra of Pd/TiO₂ films, for UV region is about 375 nm and in the visible region at 473 and 505 nm, respectively, while at 425 nm was defined a broad emission band in the pure film, while the spectrum of the film with three palladium layers is different, where a wide band of low intensity is formed of two possible bands to 370 and 385 nm, and in the visible region, two bands at 469 and 505 nm are formed, the last being the most intense. The spectrum for 520 nm presents a fading that tends to zero at 600 nm. Respective emission spectra are shown in graphics. 8 and 9.

The crystal size of the samples, from XRD was estimated at $D \sim 20$ nm, which could be related to size of the bands of the UV spectra and where the films are thin (Hirai, T., et al., (2005)), it could having the effect of the confined excitons, and therefore in the charge recombination processes. Furthermore, it is known that films prepared by the sol-gel and dipping process, containing surface states and defects and also vacancies, among others, they are active agents in the possible mechanisms that generate the photoluminescence spectra (Li, Q., et al., (2009), Gao, X., et al., (2013), Liu, G., et al., (2009)a) and so are our systems that have been prepared by the sol-gel method. The main peak in the visible (505 nm) is practically the typical peak emission whose position remains fixed, although its presence depends on the ratio of anatase-rutile phases of TiO₂.



Graphic 8 Photoluminescence spectrum of the pure Pd/TiO₂ film with four emission bands, one important in the UV region and two in the visible region



Graphic 9 Photoluminescence spectra of films, pure, one, three and five layers of palladium, Pd/TiO₂, a wide band in the UV region and two emission bands in the visible region

Results and discussion

The Pd/TiO₂ films were polycrystalline with diffraction peaks corresponding to the (1 0 1), (1 0 3) and (2 0 0) planes, respectively (see graphic. 1). The peaks were indexed according to the card no. 0021-1272 for anatase phase of TiO₂. The pure Pd/TiO₂ film provided an uneven and porous morphology, and the Pd/TiO₂ films with a surface deposit of Pd, a more uniform fine grains and growth of Pd nanoparticles (EDS analysis) morphology, were obtained.

The thin films showed a morphology with very small grains, while the average grain size was in the order of 0.1 μm or less, and roughness parameters Rq = 1.16 nm and Ra = 0.886 nm from a full 1x1 μm² image, were recorded. The films showed high transmittance, with interference effects and the bandwidth of the films showed a red shift with the number of layers of palladium catalyst, 3.67 to 3.50 eV, which means in principle, best catalytically and photoluminescent properties in films with more layers of palladium. Liu, G. et al. (Liu, G., et al., (2009)a), in composites ZnO/TiO₂ systems evaluated a $E_g = 3.84$ eV, while Malagutti, et al. (Malagutti, A.R., et al., (2009)), with the percentage of Ag, modified the bandwidth E_g of Ag/TiO₂ systems, when they implemented the degradation of an aqueous solution of rhodamine B.

In the high resolution spectra of the Ag/TiO₂ systems, Malagutti, et al. (Malagutti, A.R., et al., (2009)) sets for the orbital O1s two peaks, that of 530.0 eV was associated with the Ti-O bond, while the small peak was associated with the link Ti-OH (with maximum at 532.0 eV), in our case was 530.28 eV for the main peak and possible lattice oxygen, slightly higher value, representing a somewhat different chemical environment. The signal at 533.88 eV could be associated with a group of surface carbon (Dinh, C.T., et al., (2011)) or possible oxygen adsorbed on TiO₂ surface (Liu, H., et al., (2013)). The high resolution of Pd3d spectrum shows signals associated to metallic Pd and PdO (Hotflund, G.B., et al., (2003), Brun, B., et al., (1999)).

From the graph of C/C₀ versus irradiation time (insets in graphic 6 and 7), the slope is related to the pseudo reaction constant (Malagutti, A.R., et al., (2009)), which happens to be a reaction of first order with respect to the C concentration. Fig. 7a) shows the properties of catalytic activity of Pd/TiO₂ semiconductors, for the system without palladium and film with one layer of palladium (graphic 7).

For 0, 20, 40, 60, 80, 100 and 120 min irradiation times, thus the photocatalytic property of thin Pd/TiO₂ films, whose efficiency should be improved with surface modifications with Pd, as had being reported improvements in systems such as Ag:TiO₂ (Malagutti, A.R., et al., (2009), Dinh, C.T., et al., (2011)), among others.

Films prepared are thin and the estimated crystal sizes, could be having the effect of confined excitons and therefore in the recombination processes of e⁻ and h⁺ (Hirai, T., et al., (2005)). Furthermore, it is known that films prepared by the sol-gel and dipping process, containing surface states and defects and also vacancies, among others, which are active agents in the possible mechanisms that generate the photoluminescence spectra (Li, Q., et al., (2009), Gao, X., et al., (2013)).

Conclusions

The semiconductor Pd/TiO₂ thin film is grown on soda-lime substrates using the sol-gel process and repetitive dives. The films have the crystal structure of the anatase phase of TiO₂, with a porous morphology in pure and pore-free and uniform in those deposited with palladium, with grain growth uniformly distributed over the surface of the films, the topography of the sample shows grains rounded of various sizes, but especially in very thin films, the roughness was in the order of 1.0 nm and a surface density of 42 grains/μm² was assessed, films had good optical properties with high transmittance and especially their properties of catalytic activity in the degradation of methyl orange in particular the TiO₂ system, and the corresponding to the film with one layer of Pd, with a poor catalytic response than the pure sample, the response of the samples with three and five palladium layers, was not so different.

The experimental results of the photoluminescent properties of the TiO₂ films having both emission bands in the UV and in the visible region with the well-defined band at 505 nm, which is enhanced in one order of magnitude in Pd/TiO₂ films, in particular with three deposits of palladium, relative to the pure film. In films with one and five Pd deposits, the bands in the UV attenuate their presence and the intensity of the band in the visible is diminished, especially in the film with five layers of palladium.

Factors that influence the properties of films, both catalytic and photoluminescent, are the conditions of synthesis, morphology and porosity, film thickness, concentration of the co-catalyst, atmosphere of growth in the synthesis, and especially the treatment temperature to achieve greater crystallinity of the films. Partial results presented show significant potential applications in both degradation of substances polluting water and air, as well as applications in their photoluminescent properties of these films of titanium dioxide, and surface modifications with metal as Pd, Ag, between others.

Acknowledgments

SIP-IPN Research Proyects 20141245 and 20171063, to Natzin Tirado for editing this paper and to Ing. Omar Rios Berny by recording the photodegradation and photoluminescence spectra.

References

- Brinker C. J., (1990). Sol-gel science: the physics and chemistry of sol-gel processing, Oval Road, London: Academic Press Limited.
- Brun B., Berthet A. & Bertolini J.C., (1999). XPS, AES and Auger parameter of Pd and PdO. Journal of Electron Spectroscopy and Related Phenomena, 104, 55-60.

- Chae Y.K., Park J.W., Mori S. & Suzuki M., (2013). Photocatalytic effects of plasma-heated TiO_{2-x} particles under visible light irradiation. *Korean J. Chem. Eng.*, 30 (1), 62-66.
- Chen H., Tang M., Rui Z., Wang X. & Ji H., (2016). ZnO modified TiO₂ nanotube array Pt catalyst for HCHO. *Catalysis Today*, 264, 23-30.
- Dinh C.T., Nguyen T.D., Kleitz F. & Do T-On., (2011). A new route to size and population control of silver clusters on colloidal TiO₂ nanocrystals. *Applied Materials and Interfaces*, 2228-2234.
- Gao X., Chen J. & Yuan C., (2013). Enhancing the performance of free-standing TiO₂ nanotube arrays based dye-sensitized solar cells via ultraprecise control of the nanotube wall thickness. *J. Power Sources*, 503-509.
- Ge M., Guo C., Zhu X., Ma L., Han Z., Hu W. & Wang Y., (2009). Photocatalytic degradation of methyl orange using Zn/TiO₂ composites. *Front Environ. Sci. Eng. China* 3 (3), 271-280.
- Hirai T., Harada Y., Hashimoto S., Itoh T. & Ohno N., (2005). Luminiscence of excitons in mesoscopic ZnO particles. *J. Lumin.* 112, 196-199.
- Hoflund G.B., Hoglin H.A.E., Weaver J.F. & Salaita G.N., (2003). ELS and XPS study of Pd/PdO methane oxidation catalysis. *Applied Surface Science* 205, 102-112.
- Hou J.R., Yuan C.Z. & Yang P., (2007). Nanotube composites with photocatalytic activity for degradation of ethylene blue under UV irradiation. *J. Hazard. Mate. B*, 310-315.
- Ilican S., Caglar Y. & Caglar M., (2008). Preparation and characterization of ZnO thin films deposited by sol-gel spin coating method. *Journal of Optoelectronics and Advanced Materials* 10 (10), 2578-2583.
- Keun Chae Y., Won Park J., Mori Shinsuke & Masaaki Suzuki Masaaki, (2013). Photocatalytic effects of plasma-heated TiO_{2-x} particles under visible light irradiation. *Korean J. Chem. Eng.*, 30(1), 62-63.
- Li Q., Chen Y., Zhang X., Su Y. & Jia C., (2009). Annealing effect on the morphologies and photoluminescence properties of ZnO nanocombs. *J. of Phys. and Chem. of Solids*, 70, 1482-1486.
- Liu B., Liu L-M., Lang X-F., Wang H-Y. & Lou X-W., (2014). Doping high-surface-area mesoporous TiO₂ microspheres with carbonate for visible light hydrogen production. *Energy & Environmental Science*, 7, 2592-2597.
- Liu F., Yan X., Chen X., Tian L. & Xia Q., (2016). Mesoporous TiO₂ nanoparticles terminated with carbonate-like groups: Amorphous/crystalline structure and visible-light photocatalytic activity. *Catalysis Today*, 264, 243-249.
- Liu G., Li G., Qiu X. & Li L., (2009)a. Synthesis of ZnO/titanate nanocomposites with highly photocatalytic activity under visible light irradiation. *Journal of Alloys and Compounds* 481, 492-497.
- Liu G., Yan X., Chen Z., Wang X., Wang L., Lu G. Q. & Cheng Hui-Ming, (2009)b. Synthesis of rutile-core-shell structured TiO₂ for photocatalysis. *J. Mats. Chemistry*, 19, 6590-6596.
- Liu H., Wang J., Fan X.M., Zhang F.Z., Liu H.R., Dai J. & Xiang F.M., (2013). Synthesis of Cu₂O/T-ZnOw nanocompound and characterization of its photocatalytic activity and stability property under UV irradiation. *Materials Science and Engineering B* 178, 158-166.

Liu J., Han L., Ma H., Tian H., Yang J., Zhang G., Seligmann B.J., Wang S. & Liu J., (2016). Template-free synthesis of carbon doped TiO₂ mesoporous microplates for enhanced visible light photodegradation. *Science Bulletin*, doi: 10.1007/s1434-016-1162-3.

Malagutti A.R., Maurá Henrique A.J.L., Garbin J.R. & Ribeiro C., (2009). Deposition of TiO₂ and Ag/TiO₂ thin films by the polymeric precursor method and their application in the photodegradation of textile dyes. *Applied Catalysis B: Environmental* 90, 205-212.

Murphy A.B., (2007). Band-gap determination from diffuse reflectance measurements of semiconductor films, and application to photoelectrochemical water-splitting. *Solar Energy and Solar Cells* 91, 1326-1337.

Nejand B.A., Sanjabi S. & Ahmadi V., (2010). The effect of sputtering gas pressure on structure and photocatalytic properties of nanostructured titanium oxide self-cleaning thin film. *Vacuum* 85, 400-405.

Patcharee J., Pongsaton A., Sumentha S. & Tanakorn R., (2012). Surface and photocatalytic properties of ZnO thin film prepared by sol-gel method. *Thin Solid Films* 520, 5561-5567.

Wang F., Li F-L., Xu M-M., Yu H., Zhang J-G., Xia H-T. & Lang J-P., (2015). Facile synthesis of a Ag(I)-doped coordination polymer with enhanced catalytic performance in the photodegradation of azo dyes in water. *J. Materials Chemistry A*, 3, 5908-5916.

Xin B., Wang P., Ding D., Liu J., Ren Z. & Fu H., (2008). Effect of Surface on Cu-TiO₂

Renewable energy potential in the Usumacinta watershed: Status and opportunities

PAMPILLÓN-GONZÁLEZ Liliana†, SARRACINO-MARTÍNEZ Omar, HERNÁNDEZ-GÁLVEZ Geovanni, ORDAZ-FLORES Alejandro*.

Universidad Juárez Autónoma de Tabasco. División Académica de Ciencias Biológicas. Carretera Villahermosa-Cárdenas Km. 0.5, 86100, México

Universidad Iberoamericana, Departamento de Física y Matemáticas, Prolongación Paseo de Reforma 880, Lomas de Santa Fe, México, C.P. 01219, Ciudad de México

Received July 18, 2017; Accepted December 19, 2017

Abstract

Watersheds stand out for their rich ecosystem resources and biodiversity. In Mexico, the Usumacinta watershed leads the country's last living river, habitat of endangered species and with a high diversity of endemic aquatic species. Over recent years, it has been affected by human activities. This situation emphasizes the need to meet global energy demands through a model of sustainable development. In this context, this paper addresses a first study of the status and opportunities to use renewable energy resources in the Usumacinta watershed. Biogas and solar energy potentials were determined through data analysis, on site visits, field data collection and energy potential estimations. The biogas potential (124 TJ/y) is related to the livestock production systems established (90% extensive systems). Moreover, the region is located in areas characterized for being susceptible of flooding, high water table, salinity and sandy texture in plain. The solar potential shows a daily average solar radiation of 4.64 kWh/m²/d that is favorable for low and medium temperature thermal technology throughout the year. Exploiting these potential could power 66, 244 households, avoiding the emission of 63,042 tons of CO_{2e} in a region where the lack of electricity still persists.

Biogas, Clean Technologies, Solar Thermal, Sustainability, Vulnerability

Citation: PAMPILLÓN-GONZÁLEZ Liliana, SARRACINO-MARTÍNEZ Omar, HERNÁNDEZ-GÁLVEZ Geovanni, ORDAZ-FLORES Alejandro. Renewable energy potential in the Usumacinta watershed: Status and opportunities ECORFAN Journal-Ecuador. 2017, 4-7:26-44.

*Correspondence to Autor (E-mail: alejandro.ordaz@ibero.mx)

† Researcher contributing as first author.

1. Introduction

Watersheds stand out for their rich resources and biodiversity. They are more than the sum of patches of land and streams of water (Johnson et al., 2001). Watersheds involve the interaction among species, communities, ecosystems, but also the sharing of direct and indirect ecosystem services and resources like water, forest, springs, storage of organic matter, landscape, among others. Mexico gathers around 393 watersheds (Cotler et al., 2010).

Half of the watersheds in Mexico present from very high to extreme deterioration degree, or from low to high-pressure level of alteration (Cotler et al., 2010); and there is consider that 75% of the Mexican population is distributed along 13 watersheds. The Grijalva-Usumacinta watershed corresponds to these characteristics.

The Usumacinta watershed, located at the south of Mexico, is the ecosystem of numerous species, habitat of waterfowl populations (Ogden et al., 1988), den of threatened and endangered species (Primack et al., 1998). It is also the path of Mexico's mightiest river, "the Usumacinta" that, along with its tributaries, gives life to an impressive hydrological network.

Because of the wealth of natural resources, over recent years the Usumacinta watershed has suffered the developing human activities: extension of roads, colonization and expansion of agricultural land, and changes in land use (Manjarrez-Muñoz et al., 2007) to exploit energy and resources. The impact of these activities has yielded the decline of the forest in the region (Tudela, 1992), eutrophication and hypoxia in water bodies (Rabalais, 2004), among other consequences. Additionally, lack of access to energy services is a serious hindrance to economic and social development and must be overcome, as stated in the UN Millennium Development Goals.

The municipalities of the Usumacinta watershed are also characterized by having for the highest poverty levels in Tabasco. Major gaps exist in access to social security and basic services in housing, exceeding state and national averages. Vulnerability in these regions tends to increase due to poverty, lack of energy and weakness of local governments.

This startling situation has encouraged the need to meet global energy demands through a model of sustainable development, mainly in a state like Tabasco, in which the role of renewable energy is still limited, shadowed mainly by oil industries. In this context, the objective of this paper is to address a preliminary study of the status and opportunities on the use of renewable energy resources in the portion of the Usumacinta watershed that lies in the boundaries of the state of Tabasco, Mexico.

There are a few studies on energy vulnerability in Tabasco. In this regard, this article tries to start an investigation, finding the first answers and establishing further question for a state where 28.5% of the population live in alimentary poverty, in a country with only 43 researchers per million people (Laclete, 2012).

Understanding the renewable energy potentials and energy uses in the Usumacinta watershed will be useful as a complementary strategy to link the utilization and conservation of resources; particularly, in the establishment of an adequate management model that promotes renewable energy technology adoption, reduction of social inequalities, increased production, and redefinition of power structures (Lillo et al., 2015). Moreover, the use of renewable energy technologies, clean technologies and energy efficiency are considered promising alternatives to countries like Mexico that run large efforts to promote a sustainable development.

2. Methodology

2.1 Study area

The study area corresponds to the terrestrial portion of the lower Usumacinta watershed located in the southeast of Mexico in the state of Tabasco, which is bordered to the south and east by the Republic of Guatemala and to the north by the state of Campeche. The Usumacinta watershed (coordinates 18°61' - 17°25' N; 91°43'-91°00'W, Fig. 1) begins in Tabasco in the Tenosique's frontier with Guatemala, and extends to Centla municipality. In Tabasco, the river flows through five municipalities: Centla, Jonuta, Emiliano Zapata, Tenosique and Balancan.

The region is characterized by landscapes of plains and low hills, also areas of lakes and permanent swamps, to lesser degree valleys, canyons and mountains. The predominant climate is humid and warm humid with monthly average temperature between 22 and 28°C and precipitation from 1,800 to 2,500 mm annually.

2.2 Renewable energy potential

The approach employed to analyze the status and opportunities for renewable energy technologies in the study area is divided into two parts (Fig. 2). The first part contemplates the analysis of the current energy use and the energy trends considering a consumption perspective for the five municipalities. The second part regards the assessment of two renewable energy potentials (biogas and solar), based on the main economic activities (livestock) and energy needs in the region. Graphical representations of these potentials were generated using ArcGis 10.0 software.

Finally, as a result of the evaluations, renewable energy technological options to use these potentials to face vulnerabilities were recommended.

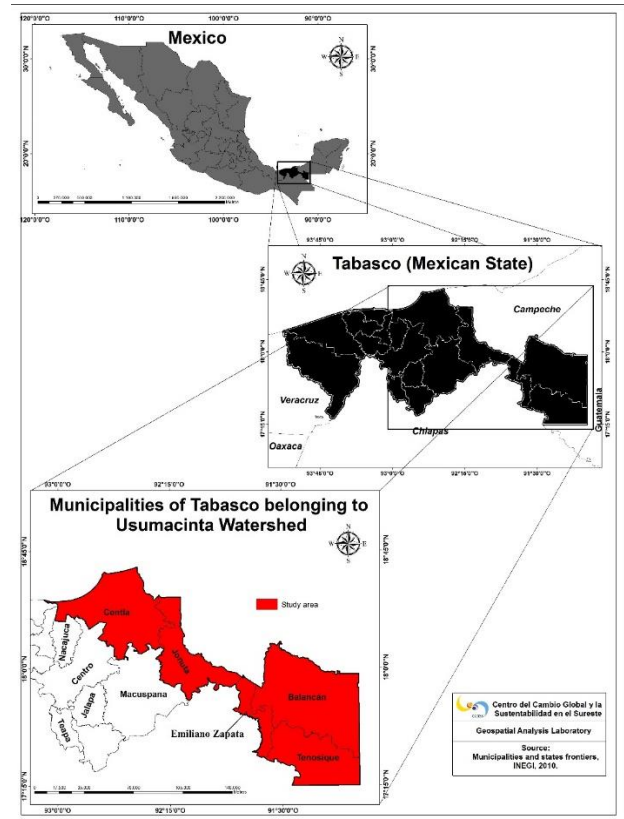


Figure 1 Location of the study area

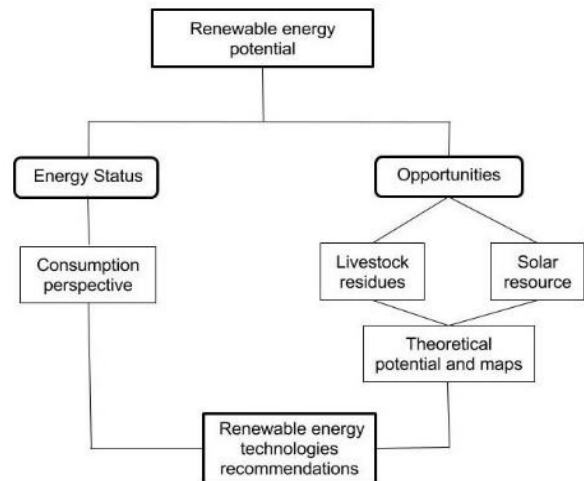


Figure 2 Flow Diagram describing the renewable energy potential studied

2.3 Biogas potential

Biogas production potential from livestock manure was calculated based on livestock population data with a modified equation from Ríos and Kaltschmitt (2013), shown in equation 2:

$$PB_{g,m,y} = \sum_{m=1}^n CG_{g,m,y} SP_g PE_g ST_g SV_g FP_g VC \quad (2)$$

Where $PB_{g,m,y}$ is the theoretical biogas potential in PJ/y, for livestock type g , municipality m and year y ; n is the number of municipalities; CG represents the livestock population (heads of animals); SP is the usable manure handling system (%); PE is the manure production (ton/heads of animals); ST is the total solids due to the manure on dry base (%); SV is the volatile solids (%); FP is the biogas production factor (m^3 /ton SV) and VC is the biogas calorific value (MJ/m^3). Values from biogas technical conversion factors used, by type of livestock, are shown in Table 1.

Type of livestock	Total solids ^a	Volatile solids ^a	Biogas production factor ^b
	— (%) —		(m^3 /ton of SV)
Cattle (Bovine)	12	80	250
Swine	8	85	375

^aSteffen et al., 1998; Fiala, 2012 .
^bBatzias et al., 2005; Wellinger et al., 2013.

Table 1 Biogas technical conversion factors used to estimate the biogas production potential from livestock manure

To estimate the usable manure handling system, a general classification of livestock production system in the region was proposed. A social evaluation through semi-structured interviews and surveys was carried out. Here, the study sample (livestock systems) comes from a non-probabilistic sampling (Snedecor and Cochran, 1981).

The information gathered (considered of exploratory level) was used to estimate the percentage of usable manure handling system according to the zootechnical function and the manure excretion rate due to the livestock weight. In this part, the animal growing stages play an important role in the assessment of biogas production by type of livestock production system. Particularly, a closer approach of manure production is derived as a function of animal weight, leading to a more reliable estimation of biogas production. Biogas production was reported in terms of energy considering that 1 m^3 of biogas is equivalent to 21.5 MJ (Batzias et al., 2005) with a methane content from 55 to 60% that generates 1.9 kWh (Tricase and Lombardi, 2009).

2.4 Solar potential

A solar irradiation database was generated to assess the solar potential and graphical representations of the potential were made. To create this database, a grid of 180 points was arranged on the five municipalities of the Usumacinta watershed. The points were geo-referenced in terrestrial coordinates with 10 km neighbor distance. Solar radiation was calculated in every point of the grid. The method used is based on Equation 3 proposed by Reddy (1970) and modified by Estrada-Cajigal and Almanza (2005) for the monthly average daily global radiation:

$$H = 0.0418K \left[\frac{(1+0.8 n/N)(1-0.2 r/m)}{0.1\sqrt{h_r}} \right] \quad (3)$$

Being

$$K = (\lambda N + \psi \cos \phi) 10^2 \quad (4)$$

Where H is the monthly average daily global radiation, ϕ is the latitude, $\lambda = 0.2/(1+0.1\phi)$ is a latitude factor, $\psi_{i,j}$ is a seasonal factor, n is the mean hours of bright sunshine per day during a month, N is the length of the day during the month, r the number of rainy days during the month, m is the number of days in the month, and h is the mean humidity per day in the month.

Data collected were processed using the platform ArcGIS 10.0, to obtain maps of average daily solar radiation for every month of the year and the annual average. Note that data had to be obtained numerically since experimental data for solar radiation are hardly available in the state. Also, this method permits to have more punctual estimates of the solar radiation.

Complementarily, communities were visited to know and understand the thermal energy needs and detect areas of opportunities; attention was paid to energy vulnerability. As a result of the above, a set of technological options were proposed. Note that, although the solar resource can be used for both thermal and photovoltaic applications, this work is focused on solar thermal technologies; the photovoltaic perspective will be matter of a further investigation.

3. Results and discussion

3.1 Current status: Usumacinta watershed

Beyond the wealth provided by the ecosystem resources and services in the Usumacinta watershed, the current unsustainable extraction patterns must come to an end. In recent years, the region has faced environmental and socioeconomic changes that have negatively affected the living ecosystems and society. For example, the local populations remain among the poorest in Mexico, being profoundly weakened by the environmental degradation.

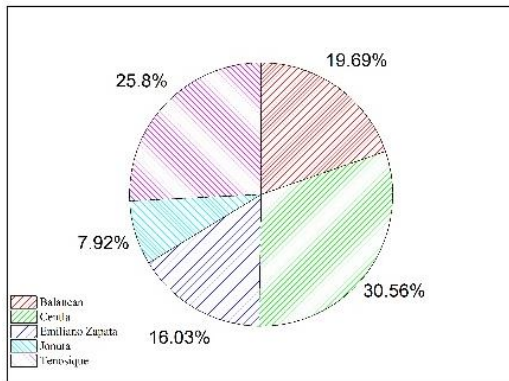
Around 3% of the total households in the study area have no electricity and the average electricity consumption per household is 4.7% lower (1768.56 kWh/household) than the rest of the country (INEGI, 2010). Regarding energy resources, traditional biomass such as wood and bagasse are the most employed in the region. In this respect, firewood in rural areas is obtained at several sites, but especially from the places with remnants of original vegetation (as forests or jungles), or regeneration zones with agroforestry systems (as cacao and coffee plantations).

Wood extraction remains a common practice today. It is partly responsible of deforestation; records of this resource extraction date from the nineteenth century (De-Vos, 1988). In the last decade, wood-saving stoves studies has been performed to attend the high marginalization in rural communities (Maserá et al., 2007).

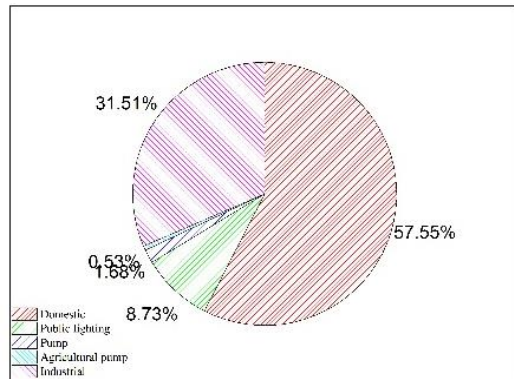
Regarding other biomass resources, livestock production figures as the main activity in rural areas, occupying 1.26 million ha, covering 67% of the state (FIRA, 2015). During and after livestock production, a large amount of waste is generated and accumulated. Most of it lacks proper handling, causing environmental, social and economic problems. Most of the local research is focused on livestock systems promotion into organic production systems; other ones suggest technologies, without taking into consideration the biogas potential (Olivares-Pineda et al., 2005).

About the solar resource, it is almost an unexplored subject in the region, although some insights has been done: the Mexican National Water Commission (CONAGUA, 2015) has five weather stations available for the Usumacinta watershed, however, they are insufficient to represent the whole region; a National Inventory of Renewable Energies has been developed by the Mexican Energy Secretariat (SENER, 2015); Hernández-Escobedo et al. (2015) have recently published their investigation on energy resources in the Gulf of Mexico.

Centla and Tenosique, municipalities of the Usumacinta watershed, are the main electricity consumers (graphic 1), with around 60% out of a total consumption of 250,693.24 MWh. Domestic and industrial sectors are the main energy consumers (graphic 2). The latter mainly because of livestock, which is the principal economic activity in rural Tabasco, that demands heat and gas for their processes (CEPAL, 2008).



Graphic 1 Electricity consumption by municipality



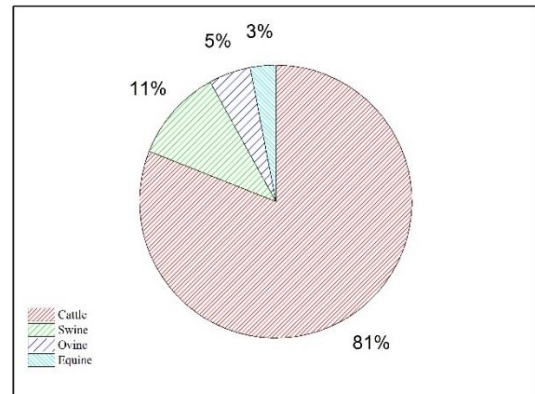
Graphic 2 Electricity consumption by sector

3.2 Livestock production in Usumacinta watershed

In the Usumacinta watershed, there has been envisioned the need to quantify the potential for the production of biogas from livestock manure, especially considering that the state plays a significant role as a national livestock producer; over 1.5 million heads of animals place Tabasco as the 7th in livestock national population of cattle (bovine) (SIAP, 2013).

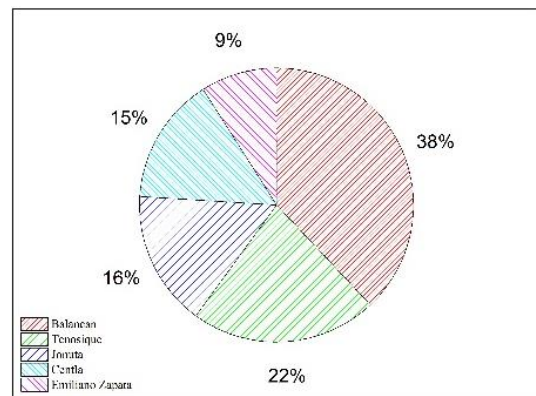
From the total of units dedicated to agricultural and forestry production in Tabasco, 41% develops activities related to livestock sector, where 81% of these livestock system are specifically dedicated to breeding and feeding cattle (Graphic 3.). That is why the importance of swine and cattle production is highlighted in this research.

This activity concentrates around 92% of the total livestock population which daily generates biomass.

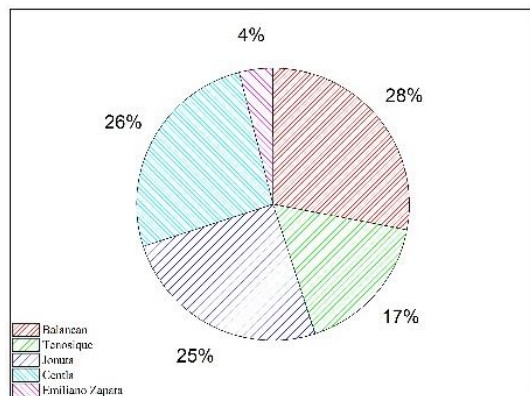


Graphic 3 Livestock population distribution in Tabasco, Mexico. (Based on data from INEGI, 2012).

Related to bovine livestock population, Tenosique and Balcanan have 117,512 and 62,784 heads of animals, respectively (Graphic 4), that represent more than 50% in the Usumacinta watershed.



Graphic 4 Livestock population distribution by municipalities of the Usumacinta watershed: bovine swine



Graphic 5 Livestock population distribution by municipalities of the Usumacinta watershed: Based on data from INEGI, 2012

The situation about the swine population is different; the region of the Usumacinta does not concentrate a relevant number of heads of animals. There are 9,024 and 6,515 heads of animals in Centla and Balancan, respectively (Graphic 5). Over 80% of swine population is concentrated in other region of the state: the “Chontalpa” region is one of them, whose municipalities have the largest livestock population.

The livestock production systems in the region in general refer to the type of management or production of animals. In this part, this classification provides a useful tool to estimate the usable organic matter. The characteristics of these production units are decisive for the excretion collection in order to be more regulated and systematized, increasing the technical feasibility for biogas production.

In this sense, the prevailing bovine livestock production system in Tabasco (90%) is free and controlled grazing (Table 2). Free grazing production system is typical in humid tropical regions, where traditional livestock railings or dual purpose (Rivas and Holmann, 2002) allows the joint production of meat and milk based on native cattle crossed with Zebu cattle and European dairy breeds (Manjarrez-Muñoz et al., 2007).

Municipality	Total population ^a	Livestock production system			
		Free grazing	Controlled grazing	Feedlot	Semi-feedlot
		—Heads of cattle—			
Balancan	117,512	77,427	32,101	1,706	5,256
Centla	44,855	25,357	8,791	587	6,249
Emiliano Zapata	29,133	18,352	7,503	994	2,178
Jonuta	50,410	40,249	3,491	386	3,849
Tenosique	62,784	36,760	19,613	1,533	3,909

^a Considering the production systems reported by INEGI, 2012.

Table 2 Livestock production systems for cattle (bovine) in Tabasco.

For the case of swine livestock, the production system is performed generally in formal farms or backyard properties. Animals produced in backyard properties, are usually for consumption as opposed to formal farms where their main purpose is marketing. On average, 73% of the swine population is confined into seeking diverse stages of production: stallion, belly, younger than 8 weeks and fattening (Table 3).

Municipality	Usable manure handling system	
	Swine	Cattle
	——(%)——	
Balancan	77,427	32,101
Centla	25,357	8,791
Emiliano Zapata	18,352	7,503
Jonuta	40,249	3,491
Tenosique	36,760	19,613
Average	73.00%	9.82%

^a Considering INEGI, 2012.

Table 3 Usable manure handling system for biogas production by municipalities

Regarding the amount of manure excreted per animal, international typical values report 8 kg manure/animal-day for the case of cattle manure and 2 kg manure/animal-day in the case of swine (Arthur et al., 2011). In order to have a better approach in the calculation of manure generated as a function of weight or zootechnical functions, Table 4 shows the data proposed to estimate the approximate manure production.

Type of livestock	Zootechnical function	Approximate weight	Manure production ^a
		— (kg) —	
Cattle	Dairy cattle (adult cow and calves younger than 7 months)	425	34
	Semental (adult bull)	532	42.5
	In development or fattening animals (breeding calves or heifer)	255	20.4
	Beef cattle (Bovine from 12 to 17 month)	297.5	23.8
	Dual purpose (cattle)	318.7	25.5
	Working animals (from 22 to 32 months)	282.5	30.6
Swine	Pig stud	180	5.03
	Sow	150	5.03
	Pigs Below 8 weeks	20	1.8
	In development or fattening	75	5.33

^a Considering a daily excretion rate of 8% of the living weight.
^b Considering a daily excretion rate of 2.93% for pig stud, 3.35% for sow, 9% for pigs below 8 weeks and 7.11% for developing or fattening animal (FIRCO-SAGARPA, 2012).

Table 4 Approximate weights and manure production (wet basis) from livestock based on the zootechnical function for type of livestock in the Usumacinta watershed

3.3 Biogas potential from livestock manure.

In Mexico, the national biomass potential from livestock residues was reported as 148 PJ/year (Libro Blanco de la Bioenergía en México, 2006). In Tabasco, the biogas potential calculated from livestock manure (bovine and swine) represents less than 1% of the national potential with 0.40 PJ/year.

The theoretical potential for biogas production from cattle residues is estimated as 124 TJ/year. The potential value for each municipality is presented in Figure 2.

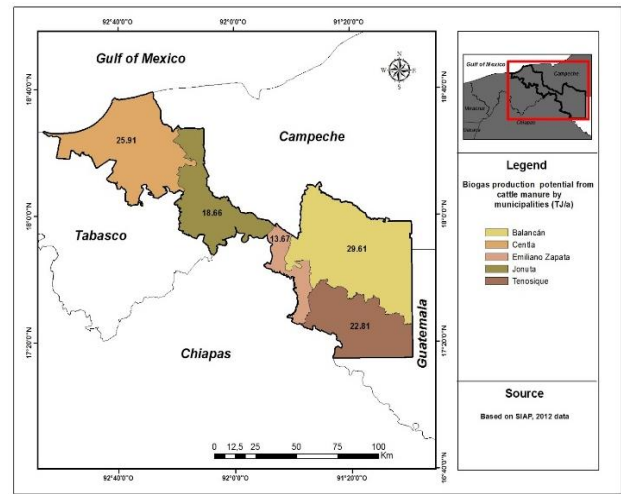
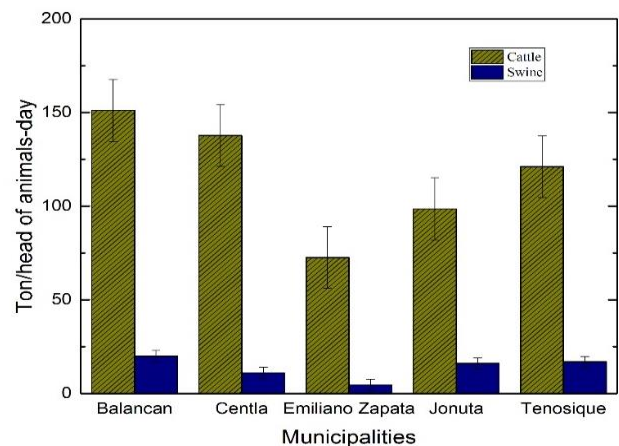


Figure 2 Biogas production potential from cattle manure (feedlot) by municipalities in the Usumacinta watershed (TJ/a)

Centla and Balancán present the greatest biogas potential with 29.6 TJ and 25.9 TJ for 2007.

This value is relatively small considering that the amount of manure livestock comes only from stables (Graphic 6); besides, these municipalities have the largest number of production units in the state, with 3,045 and 2,811, respectively (INEGI, 2012).



Graphic 6 Livestock manure production (feedlot) from cattle and swine by municipalities of the Usumacinta watershed

For the case of livestock residues, estimating the potential not only depends on the number of animals; it was found in this investigation, that despite the municipalities in the region of the Usumacinta concentrate a large number of animals in the state, the potential for biogas production from energy systems such as biogas digesters is affected by the livestock production systems in the region that are based on free grazing regime (near 90%).

A free grazing system yields not only low productivity, but also negative environmental impacts by a lack of sustainable approach, such as excessive loss of forage which leads to degradation of vegetation, increased erosion and loss of soil fertility, among others (FAO, 2014). From the point of view of the biomass resources for energy production, livestock produced in large areas difficult the feasibility to collect of organic material that would be strategic in energy production and valorization of these residues as compost or bio-fertilizers.

In this sense, it is desirable to migrate to other production systems such as intensive silvopastoral systems, as a practice that has been widely recommended for the humid tropical regions (González-Espinoza, 2013). The use of these systems will allow reducing the environmental impact from traditional production systems, increasing the capability of using the manure in a systematic way and promoting a long due sustainable development for the region.

A comparative case about the importance of livestock production systems in the biogas production is the Belgium case. Tabasco has a similar surface than Belgium (25,267 vs. 30,528 km²), but unlike Tabasco, is the intensive system of livestock production that has allowed Belgium to have a proper use of manure, and a biogas production of 341 GWh (Valbiom 2012,) covering most of its energy needs.

In the case of Tabasco, the biogas potential estimated is one tenth (35.05 GWh) compared with the production of Belgium. However, even using 10% of the livestock manure generated (referring to the manure accumulated in the stables), the energy generated could power 7,851,993 refrigerators under the assumption that 1 m³ can supply energy to a 14 ft³ system for 10 hours during a year (Samaoya, 2012), or replace the use of 27,246 tons of firewood, considering that 1 m³ prevents the use of 3.47 kg of firewood (UNESCO, 1982; Van Buren, 1974).

In relation to swine livestock residues, the biogas production potential is 13.55 TJ coming from 24,715 tons of fresh manure annually. Balancán and Tenosique have the highest potential in the Usumacinta watershed (Fig. 3); however, there are other municipalities in Tabasco, Huimanguillo (9.44 TJ) and Cardenas (7.32 TJ) with higher potentials. The swine production system, unlike bovine, has more feasibility of manure collection, since about 70% of this production is in fattening farms and stables.

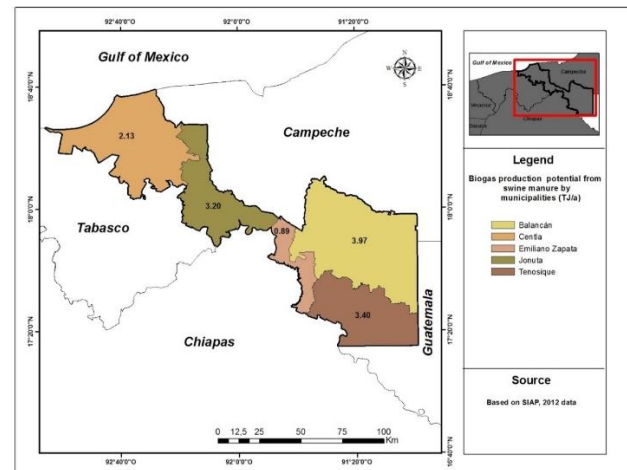


Figure 3 Biogas production potential from swine manure (feedlot) by municipalities in the Usumacinta watershed (TJ/a)

In general, as seen above in this first analysis of biogas potential, although livestock production systems are not the most suitable for the state context, proper utilization of these biofuels can mean savings in heat and power generation (Weber et al., 2012), which can help increase profitability in the agro-system. Given the relevance of the variety of applications of this bioenergy, Fig. 9 shows those sites with potential for biogas production as a priority stage.

This scenario is oriented to those sites with a relevant theoretical potential for the production of biogas that can be used to generate electricity or heat. Specifically, it considers the bovine and swine productions units indexed in the state registry, with a considerable number of animals and feasible production system for manure collection.

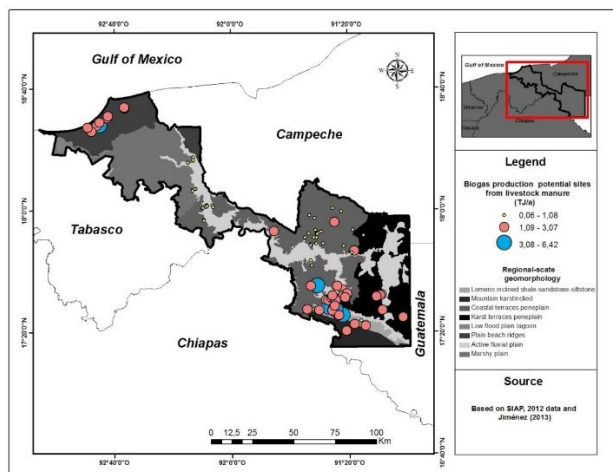


Figure 4 Sites with potential for producing biogas from livestock manure in the Usumacinta watershed in Tabasco

Casas-Prieto et al., (2009) states the requirement of at least 300 heads of animals (cattle) for a biogas production system to be profitable, while the technical specifications for the biodigesters FIRCO-SAGARPA (2012) recommends at least 100 heads of swine for profitability, too.

In this sense, sites with low potential are discarded in these priority approach; however, the possibility to install biogas systems as the “plastic bag digester” type or implementing other technologies for manure management in those production units where the number of animals is lower than recommended by specialists is not ruled out.

As a complementary analysis, the geographical location of these sites, considering the geomorphopedologic regions bounded by Jiménez-Ramírez (2013) are presented. It is noted that for Balancan and Tenosique, most sites belong to coastal and terraces peninsular zones (Figure 11); these are considered knolls in watersheds, characterized by low hills or ridges (Jiménez-Ramírez, 2013). On the other hand, the sites located in Centla are in plain areas of beach ridges considered of regular flooding. It is important to emphasize the importance of linking the extraction, exploitation and production of energy resources with environmental factors such as the geomorphopedological landscapes of Tabasco. To combine these type of criteria for the analysis of the potential of biogas is an essential exercise and it is the prelude to estimate future potentials that involve sustainability indicators.

In general, the potential sites are located in areas with geomorphological landscape conditions characterized for being susceptible to flooding, high water table, salinity and sandy texture in plain (Jiménez-Ramírez, 2013) that must be considered given that they restrict the use of agricultural land and their suitability to make deep excavations for the installation of biogas systems. Thus, installation and setup of the systems for the production of biogas must contemplate these conditions. In this sense, studies on the economic, social and environmental potential of technology are imperative to ensure sustainability. Finally, about manure uses and final disposal is not different from the current management of livestock residues in other states in the country.

Derived from the social assessment, it was found that 78% of producers interviewed dumps the livestock manure directly on the soil around their stalls; 20% use the livestock manure to produce a fertilizer (non-commercial) and 2% use to produce an enriched food to others animals. Most of the producers interviewed shows interest in environmental improvement; however, they are unaware of any applicable technology.

3.4 Technological options for manure management

One of the most common practices related to livestock manure management in the study is the direct disposal on the soil without any use. Studies show that physicochemical composition on soil can be affected by the exacerbated application of livestock manure directly, causing changes in salt content, mainly affecting water bodies, producing leach that reach groundwater and contributing to release greenhouse gases (Pampillón-González et al. 2014), (FAO, 2006).

Considering this situation, some recommendations about manure management technologies are given according to the type of process (Fig. 5). Biological processes are considered a promising technology for the region, for example composting and the use of biodigesters that can be a viable option for the use of waste in energy generation alternative.

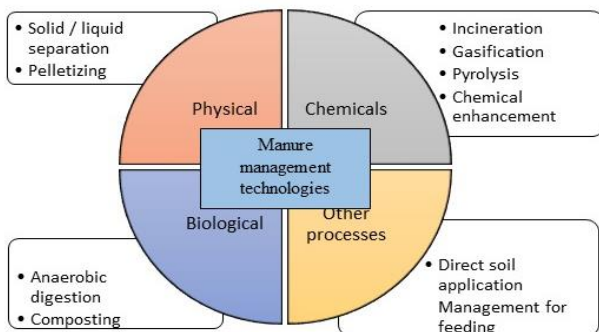


Figure 5 Technologies for the management of livestock manure. Modified from the guide for the selection of technologies for manure management (Porter et al., 2010)

3.5 Solar thermal

The maps obtained for the average daily solar radiation for the highest and lowest solar radiation months, and the yearly solar radiation maps are presented. Figure 6 shows the global average daily solar radiation (kWh/m²/d) for the month of August. The average radiation is 5.26 ± 0.03 kWh/m²/d. It is August the month with highest solar radiation during the year, with relatively small variations. This value is above the national annual average of 5 kWh/m²/d (CONUEE, 2014), surpassed in four months, though the annual average of Tabasco is lower. For the month of August, Centla and Jonuta share the highest average daily solar radiation while Balancán's northeast has the lowest.

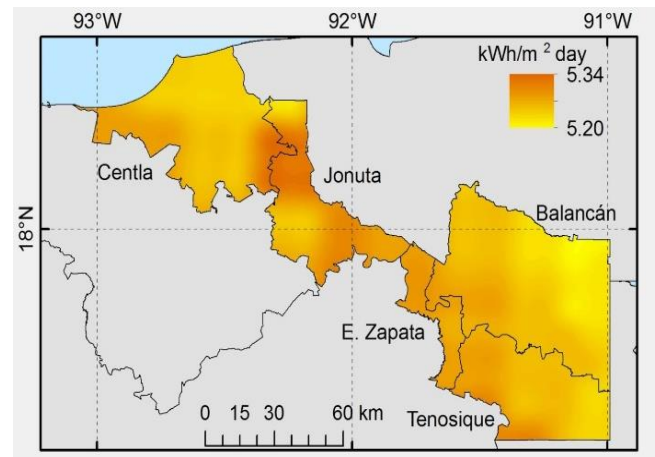


Figure 6 Average daily solar radiation (kWh/m²/d) for August in the Usumacinta watershed in Tabasco, Mexico

Figure 7 shows the global average daily solar radiation (kWh/m²/d) for December, with an average of 3.66 ± 0.07 kWh/m²/d, which categorizes as the lowest solar radiation month during the year. There are negligible variations in the region, except for the Southwest of Centla with slightly higher average. These levels of radiation can be useful for low temperature applications like water heating for homes, laundry or preheating.

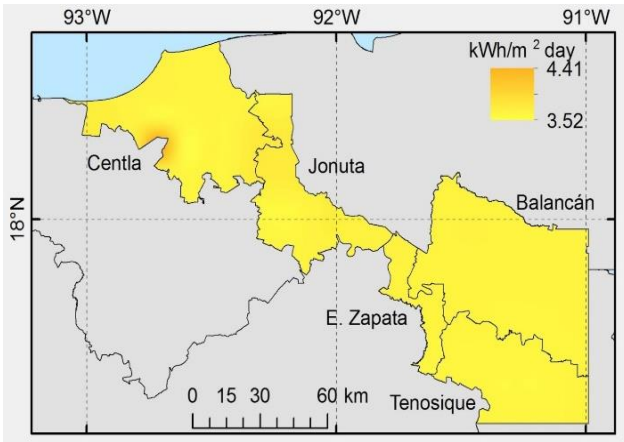


Figure 7 Average daily solar radiation (kWh/m²/d) for the month of December, for the five municipalities of the Usumacinta watershed in Tabasco, Mexico

The yearly average daily solar radiation is shown in Figure 13. The annual average is 4.64±0.53 kWh/m²/d; this value is consistent with data from the Mexican Energy Secretariat (CONUEE, 2014), that estimates it below 4.7 kWh/m²/d. The municipalities of Centla and Jonuta show the highest annual average daily solar radiation, while Tenosique has the lowest. With these levels of irradiation, medium and low temperature technologies can be thought as strategies to deal with thermal energy needs presented in the Usumacinta watershed.

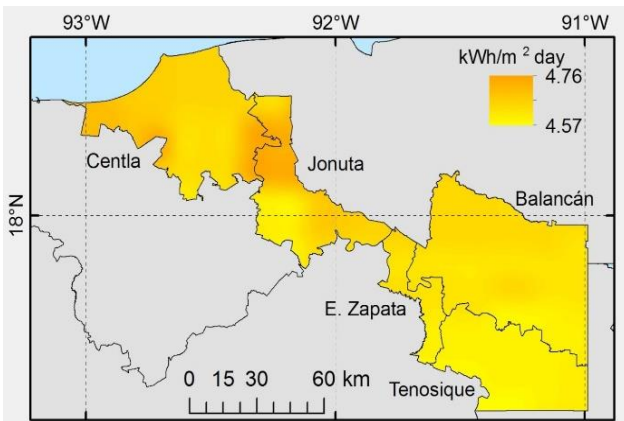
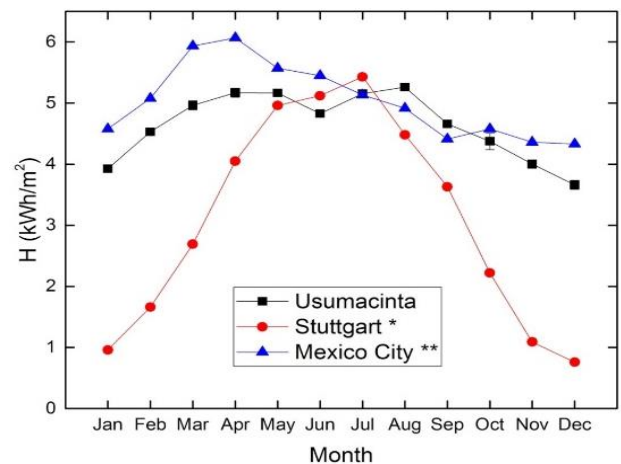


Figure 8 Yearly average of the daily solar radiation (kWh/m²/d). Data for the five municipalities of the Usumacinta watershed in Tabasco, Mexico

To have a broader perspective, it is important to analyze the average daily solar radiation behavior throughout the year; Figure 15 shows the monthly average daily solar radiation for a whole year. Only two months have average daily radiation below 4.0 kWh/m²/d (January and December), and other two below 4.5 kWh/m²/d (October and November). According to the Mexican Standard Normativity (NMX-ES-004-NORMEX-2010) for solar water heating thermal systems, a minimum of 17 MJ (4.7 kWh/m²/d) is required for an acceptable test. This value is reached during eight months in the Usumacinta watershed. Note however, that in other countries like Germany, with average of 3.6 kWh/m²/d (SolarGis, 2015), energy policies have led them to produce up to 6.9% of their consumption of electric energy with solar energy.

Low and medium temperature needs can be fulfilled with the use of solar technologies all year long, and high temperature applications might be implemented for seasonal use. High temperature is demanded mainly by industrial processes (heat and preheating).



Graphic 7 Monthly average daily solar radiations. Comparison of the solar radiations of the Usumacinta watershed, Mexico City and the German city of Stuttgart. *Duffie and Beckman (2013); **Hernández-Escobedo et al., (2015).

It is important to highlight that the use of solar technologies for low, medium and seasonal high temperature processes, yields economic and environmental benefits, such as savings in fuel consumption and reductions of global warming and greenhouse emissions.

3.6 Technological options for the use of the solar resource

In the state of Tabasco, only 6.6% of the population is exempt of vulnerability (CONEVAL, 2014) in the study region. The shortcomings suffered exceed the regional and national averages. Poverty reaches from 65.4% to 80.3% of the population, what makes people to spend most of their incomes in food (ENIGH Survey, 2015). These conditions reduce their access to energy. In general, the thermal needs of the population are usually satisfied with fossil fuels, like LP gas; however, the high prices of these fuels restrict the access. The thermal energy approach presented can provide a complementary access to energy services in these populations.

Below are presented the main thermal needs identified in the region and the technological proposals (Table 5). Mainly, energy needs were identified in what regards to food, health, temporary accommodation, industry and fishing.

Sector	Thermal energy needs	Thermal technologies	Benefits	Barriers	Target population*
Feeding	Cooking of corn to prepare food and drinks	Solar cookers	Reduction in use of firewood	Long cooking times, learning curve, disbelief	Over 70,000 households
Health	Sterilization and laundry	CPC, Dish concentrators	Access to sterilized equipment and cloths	Initial investment, learning curve	254
Temporary accommodation	Hot water for showers, laundry and food	Flat plate collectors	Economic savings	Initial investment	978
Industry	Pasteurization, sterilization of	Flat plate, evacuated tube collectors,	Economic savings, increase in	Disbelief, initial investment	643

	milking equipment	Dish concentrators	production, cleaner equipment		
Fishing	Refrigeration	Absorption refrigeration systems	Preservation of fish, economic savings	Learning curve, not-automated, intermittent	56
* In terms of the households and economic activities in the region of the Usumacinta watershed (INEGI, 2015).					

Table 5 Opportunity areas for the advantageous use of solar thermal technologies in the Usumacinta watershed in Tabasco, Mexico

Feeding

In Mexico, human consumption of corn reaches 22 million tons (out of a total of 30 millions). The human uses of corn in the region include the preparation of tortillas, tamales and a traditional drink called pozol; there are 123 tortilla producers (INEGI, 2015b); preparation of tamales and pozol is a common practice in the more than 70,000 households, too. Nixtamalization is an important process to prepare tortillas, which involves the corn cooking in a mixture of water and lime to improve food quality and texture (Rangel-Meza et al., 2003); tamales and pozol also need boiling, but no lime. Cooking 1 kg of corn requires around 4 L of water boiled from 90 to 120 min. The energy for this process is gotten from firewood or fossil fuels, however, solar thermal technologies can also provide energy for these purposes. Solar cookers are used to prepare foods that involve some kind of cooking. There are primarily two types: Fresnel-Dish and box solar cookers (del-Río-Portilla et al., 2010).

Health

Private practice is common in the Mexican health system; sterilization is of primary importance for physicians and dentists who usually do not have the appropriate equipment. Proper sterilization requires 121 °C and from 137.9 to 220.6 kPa (20 - 32 psi) for times between 3 and 30 min (Brown and Merritt, 2003).

Previous studies reveal the relevance of solar sterilizers in introducing quality standards in areas with high degrees of marginalization and vulnerability (Young, 2012; Boubour et al., 2014); in the Usumacinta watershed, susceptible to floods or power shortage, this kind of technology increases adaptation, and minimizes risks of infection.

Temporary accommodation

There are 978 economic activities in the Usumacinta watershed devoted to temporary accommodation (INEGI, 2015b). The technology of flat solar collectors for water heating in Mexico has reached maturity, and potential of savings in Hotels has been previously studied (Delgado and Campbell, 2013).

Fishing and industry

There are 275 manufacturing industries in Tenosique and Balancan (INEGI, 2015b), standing those of milk production. Freezing to -25°C is a need for the 56 economic activities in the region dealing with agriculture, animal breeding and exploitation, forestry, fishing and hunting. Several technologies as flat plate, evacuated tubes or dish solar collector, integrated to the pasteurization process can be efficiently used in dairy industries (Ray and Jain, 2014; Dobrowsky, 2015).

For the case of fisheries, absorption refrigeration systems can be implemented to address this issue (Táboas et al., 2014; Sarbu and Sebarchievici, 2015); however, refrigeration challenges require studies and monitoring to establish sustained and realistic scope in the region. Regarding applications of solar thermal technologies, there is often no single solution. Each challenge has to be evaluated independently to provide a technological solution that is thermally, economically and environmentally viable.

In a population with rooted customs, breaking barriers into gaining acceptance and appropriation of solar technologies (and renewable energies in general) requires diffusion of knowledge and convincing. Integration with other renewable technologies needs to be explored and exploited. Likewise, integration with conventional systems is paramount. Alternate use of technologies at the right times, good energy practices and appropriate energy efficiency assessments can produce higher income and environmental benefits.

3.7 Energy impacts

Table 6 shows the energy impacts of the biogas and solar energy potentials that were estimated for the region, in terms of equivalent number of household benefited and tons of CO_2 equivalent avoided. Over 48,000 households would benefit from using solar thermal technologies if an area of 0.001% was installed with solar technologies with 50% of efficiency; additionally, micro-turbo generators and methane burners would impact in the energy consumption from over 18,000 households. The total emissions avoided would reach 63,042 tons of CO_2e per year.

These results highlight the importance to thrust on the use of renewable energies such as biogas and solar thermal in the Usumacinta watershed. These technologies can reduce the emission of greenhouse gases, mitigate and improve energy security, not to say support adaptation and reduce vulnerability, in such a discriminated region. The information generated is relevant to help in the design of local public policies, overall to improve a sustainable alternative model in the Usumacinta watershed. In this respect, this and further studies are aimed to set the basis of an integral research that involves environmental, economic and social aspects.

Renewable energy potential	Available energy ^a	Technologies ^a	Benefits	Equivalent Households ^b	Tons of CO ₂ e Avoided ^c
Solar	66 EJ/y	Type-Dish Stirling Generators. Photovoltaic panels. Flat plate collectors.	Reduction in use of firewood production of heat and electricity	48,151	45,824
Biogas	124 TJ/y	Micro-turbo generators, Methane Burners		18,093	17,219
Total				66,244	63,042

^a Consider the 0.001% of the energy available in the area studied, 50% of final efficiency for solar equipment's & the use of all the biogas at 100% efficiency.
^b Considering 1.90372 MWh/household/year (INEGI, 2013)
^c 0.4999 TCO₂e/MWh for the 2013 (<http://geimexico.org/factor.html>)

Table 6 Energy impacts of the renewable energy potential evaluated

4. Acknowledgments

We would like to thank CADER-SAGARPA governmental offices for providing the livestock productions units database. The technical assistance from M.Sc. Candelario de la Cruz Peralta and Dario Chablé Arias. To CONACYT for the grant received in order to carry out the project "Incorporación de maestros y doctores a la industria para fomentar la competitividad y la innovación" 2014. PROY-C-662/2014 CONACYT

5. Conclusions

The current research shows the biogas and solar potential from the five municipalities of the Usumacinta watershed in Tabasco, Mexico. Based on the methodology proposed and data generated, a biogas (from livestock residues) and solar potential of 124 TJ/y and 66 EJ/y were estimated, respectively. It is important to note that these potential are theoretical:

To actually account the real potential in each case, they must meet real operating conditions, geomorphologic conditions, state of the art of the technology, economic, feasible and, in general, sustainability criteria. Geo-referenced maps were generated to show the spatial and temporal distribution of the potentials in the study region. The biogas production potential found is considered low and is directly influenced by the livestock production systems.

However, there are biological-based technologies such as composting or biodigester that are viable alternatives to the use of livestock residues technologies in the region. The daily average solar radiation potential of 4.64 kWh/m²/d is suitable for the use of low and medium temperature applications throughout the year. Important areas were identified for applications in different sectors (feeding, health, temporary accommodation, industry and fishing) that could be met with a set of solar concentrators, flat plate and evacuated tube collectors. Areas of opportunity for using biogas and solar thermal technologies were assessed, paying special attention to the situation of vulnerability (for energy) of the inhabitants of the study region.

The information obtained in this research seeks to provide elements for the analysis and design of energy policies for local planning; also to promote saving measures and technical proposals that will permit to generate opportunities, improve life quality, and preserve the environment.

6. References

- Arthur R., Francisca Baidoo M., Antwi E. 2011. Biogas as a potential renewable energy source: a Ghanaian case study. *Renew Energ* 36:1510-1516.
- Batzias F. A., Sidiras D. K., Spyrou E. K. 2005. Evaluating livestock manures for biogas production: a GIS based method, *Renew Energ*, 30: 1161-1176.

Boubour J., Le-Herissier B., Schuler D. 2014. Food cooking, medical sterilization and ice making (adsorption process) with the "soleil-vapeur" solar thermal steam unit, <<http://jean.boubour.pagespersorange.fr/bibliot/queque/four-pages.pdf>> (active October, 2015).

Brown S.A., Merritt K. 2003. Use of containment pans and lids for autoclaving caustic solutions, *Am J Infect Control*, 31 (4): 257-60.

Casas-Prieto M.A., Rivas-Lucero V.A., Soto-Zapata M., Segovia-Lerma A., Morales-Morales H.A., Cuevas-González M.I. Keissling-Davison C.M. 2009. Estudio de factibilidad para la puesta en marcha de los digestores anaeróbicos en establos lecheros en la cuenca de delicias, Chih. Cuarta época. Año XIII. Volumen 24. enero-junio.

CEPAL, 2008. Tabasco: Características e impacto socioeconómico de las inundaciones provocadas a fines de octubre y a comienzos de noviembre de 2007 por el Frente Frío N° 4, Comisión Económica para América Latina y el Caribe/CENAPRED. Chile <www.eclac.org>. CONAGUA, 2015. Comisión Nacional del Agua <<http://smn.cna.gob.mx/emas/>> (active October, 2015).

CONUEE, 2014. Comisión Nacional Para el uso de la energía Eléctrica, 2014. <http://www.conuee.gob.mx/wb/CONAE/que_es_la_energia_solar> (active October, 2015).

Delgado R., Campbell H.E. 2014. Adaptation and Sizing of Solar Water Heaters in Desert Areas: For Residential and Hotels, *Energ Procedia*, 57: 2725-2732.

del-Río-Portilla J.A., Tapia Salinas S., Jaramillo Salgado O.A. 2010. Cocedores solares, *Revista Digital Universitaria*, 11 (10).

De-Vos, J. 1988. Oro verde: la conquista de la selva lacandona por los madereros tabasqueños 1822-1949. Fondo de cultura Económica, CIESAS, México, D.F.

Dobrowsky P.H., Carstens M., De Villiers J., Cloete T.E., Khan W. 2015. Efficiency of a closed-coupled solar pasteurization system in treating roof harvested rainwater, *Sci Total Environ*, 536:206-214.

Duffie J. A., Beckman W.A. 2013. *Solar Engineering of Thermal Processes*, 4th Edition, Wiley.

ENIGH, 2015. Encuesta Nacional de Ingresos y Gastos de los Hogares (ENIGH) 2014.

Estrada-Cajigal Ramírez V.; Almanza-Salgado R. 2005. Irradiaciones global, directa y difusa, en superficies horizontales e inclinadas, así como irradiación directa normal, en la República Mexicana, UNAM.

FAO, 2006. *Livestock's long shadow: Environmental issues and options*. ISBN 978-92-5-105571-7. Rome, Italy. pp. 377

FAO, 2014. *Regional Perspectives*. URL: <http://www.fao.org/americas/perspectivas/ganaderia/en/>

Fiala M. 2012. *Energía da biomasse agricole*, Maggioli Editore.

FIRA, 2015. Red de Valor: Bovino de Carne en el estado de Tabasco. Residencia estatal Tabasco <<http://www.fira.gob.mx/OportunidadNeg/DetalleOportunida.jsp?Detalle=17>> (active August, 2015).

FIRCO-SAGARPA, 2012. Curso sobre especificaciones técnicas para el diseño y construcción de biodigestores en México. Morelos, México.

Hernández-Escobedo Q., Rodríguez-García E., Saldaña-Flores R., Fernández-García A., Manzano-Agugliaro F. 2015. Solar energy resource assessment in Mexican states along the Gulf of Mexico, *Renewable and Sustainable Energy Reviews*, 43:216-238.

INEGI, 2010. Anuario Estadístico y geográfico de Tabasco 2010. Aguascalientes, Aguascalientes. México.

INEGI, 2012. Panorama Agropecuario en Tabasco 2007-2012: Censo Agropecuario 2007. Instituto Nacional de Estadística y Geografía, 2012.

INEGI, 2015^a. Instituto Nacional de Estadística y Geografía, <<http://www.inegi.org.mx/>> (active July, 2015).

INEGI, 2015b. DENEUE Directorio Estadístico Nacional de Unidades Económicas <<http://www.inegi.org.mx/est/contenidos/proyectos/deneue/presentacion.aspx>> (active August, 2015).

Jiménez-Ramírez R. 2013. Clasificación y caracterización de suelos de Tabasco con base en el enfoque geomorfopedológico. Tesis de maestría en Ciencia. Colegio Postgraduados. <http://hdl.handle.net/10521/2213>

Li X.Z., Zhao Q.L., Hao X.D. 1999. Ammonium removal from landfill leachate by chemical precipitation. *Waste Management* 19(6):409-415.

Libro Blanco de la Bioenergía 2006. Red Mexicana de Bioenergía. <<http://www.rembio.org.mx/wp-content/uploads/2014/10/libro-blanco-bioenergia-2006.pdf>>

Lillo P., Ferrer-Martí L., Fernández-Baldor A., Ramírez B. 2015 A new integral management model and evaluation method to enhance sustainability of renewable energy projects for energy and sanitation services, *Energy for sustainable development* 29: 1-12.

Manjarrez-Muñoz B., Hernández-Daumas S., de-Jong B., Nahed-Toral J., de-Dios-Vallejo O.O., Salvatierra-Zaba E.B. 2007. Configuración territorial y perspectivas del ordenamiento de la ganadería bovina en los municipios de Balancán y Tenosique, Tabasco. *Investigaciones Geográficas. Boletín del Instituto de Geografía, UNAM*, 64: 90-115.

Masera O., Edwards E., Armendariz C., Berrueta V., Johnson M., Bracho L., Riojas H, Smith K. 2007. Impact of "Patsari" improved cookstoves on Indoor Air Quality in Michoacan, Mexico. *Energy for sustainable development* 11(2):45-56.

NMX-ES-004-NORMEX-2010. Mexican Standard Normativity. Energía solar: evaluación térmica de sistemas solares para calentamiento de agua-método de prueba.

Ogden J.C., Knoder C.E., Sprunt A. 1988. Poblaciones de aves acuáticas coloniales en el Delta del Usumacinta, México, In: INIREB División Regional Tabasco, Gobierno del Estado de Tabasco, Ecología y conservación del delta de los ríos Usumacinta y Grijalva (Memorias), Villahermosa, México, pp. 569-574.

Olivares-Pineda R., Gómez-Cruz M.A., Meraz-Alvarado M del R., 2005. Potencial de conversión de explotaciones ganaderas convencionales a sistemas de producción orgánicos en el estado de Tabasco. *Técnica pecuaria en México*, septiembre-diciembre, año/vol.43, número 003. Instituto Nacional de Investigaciones Forestales, Agrícolas y Pecuarias. México, México pp.361-370.

- Pampillón-González L., Paredes-López O., Hernández-García G., Luna-Guido M., Ruíz-Valdiviezo V., Dendooven L. 2014. Greenhouse gas emissions and characteristics of wheat (*Triticum ssp. L*) amended with anaerobically digested pig slurry for biogas production. *Journal of Biotechnology*. (185S) S37-S125.
- Porter J., Davis J., Hickman D. 2010. Selection Guidance for Manure Management Technologies. International Symposium on Air Quality and Manure Management for Agriculture. Dallas, TX. September 13-16, 2010. United States Department of Agriculture (USDA) and Natural Resources Conservation Services (NRCS).
- Primack, R.B., Bray D., Galleti H.A., Ponciano I. 1998. *Timber, Tourist and Temples: Conservation and Development in the Maya Forest of Belize, Guatemala and Mexico*, Island Press, Washington, D.C.
- Ray C., Jain R. 2014. Chapter 3 - Solar Pasteurization, In *Low Cost Emergency Water Purification Technologies*, edited by Chittaranjan Ray, Ravi Jain, Butterworth-Heinemann, Oxford, Pages 31-53, ISBN 9780124114654
- REN21. *Renewables 2010. Global status report*. Paris; REN21.
- Samaoya Svetlana. 2012. *Guía implementación de sistemas de biodigestión en ecoempresas*, Tegucigalpa, SNV.
- Rabalais, N.N. 2004. Hipoxia en el Golfo de México, In *Book: Diagnóstico ambiental del Golfo de México*, Vol. II, Instituto Nacional de Ecología, México, pp. 773-790.
- Rangel-Meza E., Muñoz-Orozco A., Vázquez-Carrillo G., Cuevas-Sánchez J., Merino-Castillo J., Miranda-Colín J., 2004, Nixtamalización, elaboración y calidad de tortilla de maíces de Ecatlán, Puebla, México. *Agrociencia* 38: 53-61. 2004. Essay.
- Reddy S. J., 1971. An empirical method for the estimation of total solar radiation, *Solar Energy*, 13 (2):289-290.
- Ríos M., Kaltschmitt M. 2013. Bioenergy potential in Mexico –status and perspectives on a high spatial distribution. *Biomass Conversion and Biorefinery* 3:239-254.
- Rivas L., Holmann F. 2002. Sistemas de doble propósito y su viabilidad en el contexto de los pequeños y medianos productores en América Latina tropical. En *curso y Simposium Internacional. Actualización en el manejo de ganado bovino de doble propósito*. UNAM. Martínez de la Torre, Veracruz, México. pp. 13-53.
- Sarbu Ioan, Sebarchievici Calin. 2015. General review of solar-powered closed sorption refrigeration systems, *Energy Conversion and Management*, 105: 403-422
- SENER, 2015. *Inventario Nacional de Energías Renovables*, <<http://inere.energia.gob.mx/publica/version3.7/>>, (active October, 2015).
- SIAP, 2013. *Población ganadera con información de las delegaciones SAGARPA*.
- Snedecor W.G., Cochran G.W. 1981, *Métodos estadísticos*, CECSA, México.
- SolarGis, 2015. *Solar Database according to the international comparison*. <www.solargis.com>, (active October, 2015).
- Steffen R., Szolar O., Braun R. 1998. *Feedstocks for anaerobic digestion*. Institute for Agrobiotechnology Tulln. University of Agricultural Sciences Vienna.
- Laclete, J. 2012. *Tabasco, Diagnóstico en Ciencia, Tecnología e Innovación*. Foro Consultivo Científico y Tecnológico.

Táboas F., Bourouis M., Vallès M. 2014. Analysis of ammonia/water and ammonia/salt mixture absorption cycles for refrigeration purposes in fishing ships, *Applied Thermal Engineering*, 66 (1–2): 603-611.

Tricase C., Lombardi M. 2009. State of art and prospects of Italian biogas production from animal sewage: technical-economic considerations, *Renewable Energy* 34: 477-485.

Tudela F. 1992, *La Modernización forzada del trópico: el caso tabasqueño. Proyecto integrado del Golfo. El colegio de México, CINVESTAV, IFAIS, UNRISD, México*, pp. 136-147.

UNESCO, 1982, *Consolidation of information. Pilot edition. General Information Programme and Universal System for Information in Science and Technology*. Paris, France.

Valbiom 2012. Wallonian Biogas association/EDORA- Federation of renewable energies/Biogás E-Anaerobic digestion platform of Flanders. <<http://www.valbiom.be/files/library/Docs/Biomethanisation/Profile-biogaz-de-la-Belgique-EN-2012.pdf>>

Van Buren. 1974. *A chinese biogas manual: popularising technology in the countryside*. Intermediate Technology Publications, London.

Weber B., Pampillón-González L., Torres Bernal M. 2012. *Producción de biogás en México: estado actual y perspectivas. Cuaderno Temático No. 5. Editorial Red Mexicana de Bioenergía, A.C.* pp. 47 ISBN: 978-607-96084-1-5.

Young A. 2012. *Solarclave / Nicaragua, A solar powered autoclave to sterilize medical instruments in offgrid and rural clinics* <<https://d-lab.mit.edu/scale-ups/solarclave>> (active August, 2015).

Wellinger A., Murphy J., Baxter D. 2013. *The biogas handbook: science, production and applications*.

Lectins Gal/GalNAc from medicinal plants extracts with gastrointestinal activity have effects on the biological activity of *Escherichia Coli* O157H7

GILES-RIOS, Héctor^{1†}, COUTIÑO-RODRIGUEZ, Rocío^{1*}, ARROYO-HELGUERA, Omar¹, HERNÁNDEZ-CRUZ, Pedro²

¹Universidad Veracruzana. Instituto de Salud Pública, Av. Luís Castelazo Ayala S/N. Xalapa, Veracruz, México. C.P. 9102.

²UNAM-UABJO. Genómica, Proteómica y Glicobiología del cáncer. Centro de Investigación Facultad de Medicina. Facultad de Medicina Oaxaca Mex. CP 68000UABJO

Received July 18, 2017; Accepted December 19, 2017

Abstract

In this work we characterized lectins from different gastrointestinal medicinal plant extracts (*Hyptis mutabilis*; *Zebrina pendula*; *Salvia officinalis*; *Mentha piperita*; *Melissa officinalis*; *Ruta chalepensis*; *Psidium guajava*; *Foeniculum vulgare*; *Chenopodium ambrosoides*; *Marrubium vulgare*; *Matricaria chamomilla*; *Heteroteca indulis*). We found by hemagglutination test (HA) that all protein plant extracts (PE) recognized all analyzed blood types A, B, and O determinant antigens, but highly specificity to type B, which means Gal recognized. The results shown that majority proteins from all PE migrate around 14 to 250 kDa, and all has a common pattern bands around 14 to 21 kDa. In blood type B and A the principal sugars recognized by PE were principally Gal, GalNAc, Gal N, Neu5Ac and GlcNAc, suggesting the presence of at least RIP, Gal/GalNAc o CHI type of lectins. In addition to this, most the PE inhibited *E. coli* O157H7 hemagglutination with the same specificity in all 3 blood types A, B and O, better that their HA activity, and also PE from *Hyptis*, *Manrrubium*, *Zebrina*, *Mint* and *Foeniculum* shown highly activity in *E. coli* O157H7 agglutination, suggesting a recognition to the bacteria with exception of *Salvia*, *Chenopodium* and *Ruta* that were cytotoxic to it. Adhesion to cells HELA was not detected because most PE in the presence of the bacteria were toxic to cells. For the first time we detected that most plant PE have lectin activity to Gal and acytaled sugars that recognized highly group B and inhibited *E. coli* O157H7 hemagglutination and induces toxicity and it is agglutination also they recognized xylose sugar, suggesting proteoglycan participation in those mechanisms.

Lectins, *E. coli* O157H7, Medicinal plants, Gal/GalnAc type lectins

Citation: GILES-RIOS, Héctor, COUTIÑO-RODRIGUEZ, Rocío, ARROYO-HELGUERA, Omar, HERNÁNDEZ-CRUZ, Pedro. Lectins Gal/GalNAc from medicinal plants extracts with gastrointestinal activity have effects on the biological activity of *Escherichia Coli* O157H7. ECORFAN Journal-Ecuador. 2017, 4-7:45-59.

*Correspondence to Autor (E-mail: ecoutino@uv.mx)

† Researcher contributing as first author.

Introduction

The *E. coli* O157H7 is the microbial agent involved in hemorrhagic enteritis diarrheic disease and, as other enteropathogenic *E. coli*; it has a fimbrial 1 adhesin, and adherent factors, such as intimin, Shiga-like toxin I (SLTI) and II (SLTII). All virulent and pathogenic factors involved in this disease were characterized by the hemolytic uremic syndrome developed in about 2 to 7% of the cases. This disease also affects children from one to five years old, and specially, those under one year (82%). With a mortality range from 10% to 30%, causing damage, specially, chronic renal failure, hypertension, microangiopathic anemia, and thrombocytopenia. In Argentina and Chile, the HUS is one of the main causes of acute renal failure in children under 4 years old [1-5].

E. coli O157H7 is epidemiologically important since it is acquired through the consumption of uncooked meal from swine and cattle. Recently in Chile, report pigs as the main source representing a public health problem, because, strains isolated from fecal samples either healthy or with disease, displayed a *E. coli* O157H7 adherence factor (EAF) than in bovines [6]. *E. coli* O157H7 is not a public health problem in México.

Several studies shown that *E. coli* normally inhabits in mammals intestines, including humans. However, some highly pathogenic bacteria causing severe diarrhea and many of them are *E. coli* varieties; enterotoxigenic, enteropathogenic, enteroaggregative, enteroinvasive and enterohemorrhagic [6]. The pathogenicity depends on many adhesive and virulent factors, such as capsules, fimbriae, toxin production and the presence of adhesins that allow adhesion in the intestinal surface. Most of them are associated with the presence of plasmids, bacteriophages and bacteria chromosomal genes [7-18].

The recognition between bacteria and epithelial cells usually occurs in the presence of glycosidic residues in the membrane capsules, in receptors or proteins that act as lectins, such as bacterial fimbriae, EAF and colonization or invasion factors of epithelial cells. The case of type 1 fimbriae which recognizes mannose and participates in the colonization, and penetration of the epithelial cells at the bottom of the intestine, before enteropathogenic *E. coli* and *E. coli* O157:H7.

Type 1 fimbriae can also agglutinate red blood cells (they are called type P fimbriae in the presence of uropathogenic *E. coli*, through the recognition of α -D-Gal (1-4)- β -D-Gal sugar residues [10-13, 19]. Another important group of adhesin is type S fimbriae, which recognizes α -sialyl-(2, 3)- β -Gal associated with glycoproteins from the extracellular matrix such as laminin. It has been reported that in enterotoxigenic *E. coli* several fimbriae factors shown lectin activity involved in adherence, through Man, GlcNac, GalNac or sialic acid (Neu5Ac) sugar recognition and their genes are located either in the chromosome or in plasmids [15]. Also, bacterial toxins such as Shiga toxin and Shiga like Toxin produced by enterohemorrhagic strains of *E. coli*, are classified as lectin type 2 RIP's.

The role of lectins in microbial pathogenesis has been extensively studied [10, 17, 19-26] and these active compounds from natural sources may prevent several process like microbial pathogenesis, toxin adhesion, bacterial agglutination, growth and cell death such as apoptosis and necrosis [26-27]. Lectins have been an important tool for oligosaccharide characterization as well as isolation of cellular populations in studies in cell regulation and also as potentially antineoplastic drugs [28]. In this work, we characterized the effects of lectins from several PE from gastrointestinal medicinal plants on the biological activity of *E. coli* O157H7 and identified the sugar involves in that recognition.

Materials and Methods

Plants

Plants with gastrointestinal effects used in this work were previously reported in Mexico by Lozoya [29] and described in table 1. All plants were bought at the local market and classified comparatively with a taxonomic guide from the National Ecology Institute (INECOL). Scientific and common names: *Hyptis mutabilis* (tropical bush mint or tapon), *Zebrina pendula* (dayflower) *Salvia officinalis* (sage) *Chenopodium ambrosioides* (wormseed), *Heteroteca indulis* (arnica), *Mentha piperita* (mint), *Matricaria chamomilla* (chamomilla), *Melissa officinalis* (melissa), *Foeniculum vulgare* (fennel) *Marrubium vulgare* (horehound) *Psidium guajava* (guava), *Ruta xalapensis* (rue)

Plant proteins extract (PE)

A total of 100g of each plant was incubated in 200 ml of petroleum ether per gram for 30 min at room temperature. After delipidation, the samples were macerated in 250 ml of phosphate buffer solution containing 10 mM of phosphate, plus 150 mM of sodium chloride at pH 7. Macerated samples were filtered using gauze, then centrifuged for 10 min at 700 rpm. To the clear supernatant, several drops of trichloroacetic acid at 10% to precipitate proteins were added, and then centrifuged for 15 min at 7000 rpm (Survall super T 21); finally, a double volume of cool acetone was also used to precipitate proteins. Each pellet was washed twice in distilled water to eliminate acid excess, and the pellets were solubilized in phosphate buffer, then aliquots (text refereed as PE) of 10 ml were stored at 0°C.

Quantification of carbohydrates and proteins

Protein quantification was done by the modified Lowry procedure, using 400 µg/ml of bovine albumin as standard. The sugar concentration was quantified by the Smith method, 400 µg/ml of glucose was used as standard.

SDS-PAGE gels

Samples (50 µg/protein well) were applied to 10 and 15% SDS-Polyacrylamide gels according to Laemmli procedure, with or without mercaptoethanol. Gels were stained with Coomassie Brilliant Blue R250. To determine molecular weight of the bands, pre-stained standards of Gibco and cross-linked hemoglobin were used, and the resulting bands were analyzed with Digital MSD 40 Science 1D program from Kodak.

Hemagglutinating activity

Erythrocytes from groups A, O, and B from healthy human donors were collected in heparinized syringes, and washed 5 times in 10 mM of sodium phosphate diluted in 150 mM of sodium chloride pH 7.4. Finally, a suspension of 5% of red cells was prepared to test lectin activity through hemagglutination (HA) activity as Coutiño [22] described. The hemagglutinating capacity of the extracts was evaluated using 25 µl of extracts mixed with 25 µl of 5% red cells suspension from groups A, B and O, and added with 50 µl of phosphate buffer (10 mM sodium phosphate and 150 mM sodium chloride pH 7.4).

Then, double dilution was performed on microplates, in order to obtain the hemagglutination titer after one hour incubation at room temperature or, 30 min at 35°C, the hemagglutination titer was expressed as the highest dilution showing detectable agglutination. The hemagglutinating units were expressed as the minimum concentration of the protein necessary to obtain agglutination (HA units) and the specific activity of hemagglutinating is the number of HA units per mg of protein.

Inhibition of hemagglutination by sugars

The specificity of the lectin was determined by HA competition assay using sugar standards as references: Monosaccharides: GalNac (N-acetyl-D-galactosamine), Gal (Galactose), Fuc (L-fucose), Glc Nac (N-acetyl D glucosamine), Man (mannose), Glu (glucose), Neu5Ac (neuraminic or sialic acid), Xyl (Xylose), GalN (Galactosamine) and GlcN (glucosamine) at 1 mM (Sigma Chemicals, Saint Louis, Missouri).

Double serial dilutions using the last titer or 50 µg from each PE that can produce HA was incubated for 30 min. with 25 µl of 2% of red cells suspension. The HA inhibition was determined by the lost of agglutination and by OD values at 650 nm, based on control.

Bacterial growing cells

The *E. coli* 0157:H7 bacteria was cultured in Eosin Methylene blue agar (EMB) for 24 hrs at 37°C. Then, colonies were taken out and placed in 3 ml of PBS, 1 ml of this solution was placed EMB agar plates, and incubated for 48 hrs at 37°C (1 OD 650 nm or at 2 on the Marfan scale). Finally, this culture was diluted in order to obtain 2% of bacteria solution that was used by *E. coli* hemagglutination and agglutination assays.

Hemagglutinating activity of *E. coli* 0157:H7

The method used for hemagglutinating activity was according to Evans [30] A total of 25 µl of *E. coli* 0157:H7 solution at 2% were mixed with 25 µl of erythrocytes at 2%, and added with PBS, in order to complete a volume of 100 µl in plates of 96 cells. Then the plates were incubated at room temperature, the bacterial agglutination was identified directly by adding to each sample some drops of acridine orange stain to identify the ring of the agglutination without microscopy (corroborated by Nikon stereoscopic microscopy observation). Spectrophotometer values from the Spectra Max at 625 nm were used, the value of OD changes when bacterial agglutination exists.

Hemagglutination activity assay and inhibition by sugars

This assay was according to Evans [30] and the sugar-binding lectin specificity was identified by competition experiments using serial double dilutions with 1 mM of sugar standards.

Hemagglutination activity Assay and inhibition by lectins

A total of 25 µl of *E. coli* 0157:H7 solution at 2% was mixed with 25 µl of erythrocytes at 2%, and with 50 µg/ml of protein extract in a final volume of PBS phosphate buffer solution. The inhibition of *E. coli* hemagglutination activity was detected as described above. The inhibition could indicate that lectins from extract compete for the same carbohydrate, which *E. coli* recognized in the red cells attachment.

Specific Activity of plant extracts in agglutination of *E. coli* 0157:H7

Bacteria were grown in a culture broth at one OD on a scale from 1 to 625 nm or 2 on the Marfan scale and then diluted in order to obtain 4.8×10^6 cells/mL. After, were placed 50 µl/well and then 50 µl of PE. Double dilution was performed and then was incubated for 30 min at room temperature. The bacterial agglutination was identified as described above.

Activity from plant PE in the adhesion of *E. coli* 0157H7 and their toxicity to HELA cells

The HELA cells were donated by Dr. Alfonso Gonzalez Noriega from the Institute of Biomedical Research of the National Autonomous University of México; they were kept in a moist atmosphere with 5% of CO₂ in a BEM Dulbecco medium with 10% of bovine fetal serum (Difco) without antibiotics). Three T75 confluent flasks were trypsinized for sowing about 500,000 cells in cover slips, 3 per Petri dish, for 24 hrs. of incubation in a medium free of antibiotics.

Subsequently, they were treated with 400 µg/mL of proteins from the different extracts in the presence of 480,000 bacteria/mL, incubated for 2 hrs washed 3 times with PBS and fixed. The data reported are from a microscopic analysis of the cover slips, in which cells with adhering and agglutinated bacteria were analysed and the total number of HELA cells per cover slip were counted. Table 6 (A y B).

The same procedure was reported with the HELA cells in Petri dishes fixed washings with PBS and after that, they were incubated with 400 µg/mL of proteins from the different extracts in the presence of 480,000 bacteria/mL, incubated for 2 hrs and washings with PBS. Subsequently nutritive agar was added to the cells in Petri dishes and they were incubated for 24 hrs, after which the units forming colonies (UFC) were counted.

Results

Characterization and identification of lectins in plants PE

The content of proteins vs carbohydrates are resumed in the Table 1 and shown low quantities of carbohydrate vs proteins in all PE. The results showed lectins activity in most of the PE measured by HA assay in blood type A, B or O, excluding chamomille PE (Figure 1). PE from tropical bushmint has the higher HA capacity in blood type B with 204, 800 units and 800 units in blood type O vs arnica with 4697 units of HA in blood type A (Figure 1).

Characterization of sugar-binding lectins

The tropical bushmint PE showed the higher specificity by Gal recognition in the blood type B. However, the other PE shows more than one titer, which suggests a different type of lectin or a monomeric form with different specificity (Table 1). Our results shown that all sugars inhibited at 15 µM HA caused by PE, (see Table 2).

In contrast, sugars displaying higher HA inhibition activity were Gal and derivatives GalNAc and GalN in 10 of the 11 PE in blood type A and Neu5Ac for blood type B and O in 5 of 12 PEs; Man, in 6 of 12 PE in blood type B; xylose, only inhibited in A and O blood type in 5 of 12. In unwashed erythrocytes GlcNAc and Neu5Ac induce hemolysis.

Molecular weight characterization of the PE

The majority of PE displays common bands, between 20-14 to 58 kDa (Table 3). Some of them presented bands with high molecular weight above 100 kDa, which may correspond to super-molecular aggregates. Few proteins migrated a similar molecular weight that the protein albumin and around of 30 kDa.

Characterization of *E. coli* 0157:H7 hemagglutination

According to Table 4, we found almost an equal affinity between *E. coli* 0157H7 and all blood types A (titer 1:32 to 1:512), B (titer 1:1 to 1:256) and O (titer 1:1 to 1:256), these data indicate that the higher affinity was with blood type A. In addition to this, *E. coli* 0157H7 HA competition assay with sugar standards demonstrated the participation with high affinity in the tree groups of Man, Glc, Fuc and Xyl in the membrane recognition between bacteria and red cells and with less affinity in the group A Gal and derivatives, in the group O Neu5A and in the group B Glc and derivatives.

Bacterial hemagglutination is mediated by fimbrial type 1, although in *E. coli* O157H7 has not been demonstrated and literature data are controversial. However, our results suggest that Man Glc, Fuc and also Xyl could be involved in bacteria adherence to red cells, as well as other fimbriae, such as P fimbriae which recognized Gal and GalNAc.

Inhibition of *E. coli* 0157H7 hemagglutination by lectin from PE

All PE inhibit *E. coli* 0157H7 hemagglutination, but only in blood type B displayed effective inhibition because also presented high HA specific activity. The most important PE for inhibited the HA of *E. coli*, were from *labiatae* family; mainly, those that showed the highest HA activity in blood type B, such as tropical bush mint, dayflower, sage and mint (Table 5). Also we report that greater part of PE showed the same specific activity in the inhibition of *E. coli* hemagglutination in all blood types (A, B and O) which suggest a bacterial recognition probably to P fimbriae.

Effect of lectins in *E.coli* 0157H7 agglutination

Our results shown that most of PE that inhibited *E. coli* hemagglutination have a high activity in *E. coli* 0157H7 agglutination (Table 5); this is confirmed by lectin activities and similar sugar recognitions (Table 2, 4). Such as the case of PE from tropical bush mint, horehound; tropical bush mint, and dayflower which present a specific activity above of 10000 units of *E. coli* agglutination, in comparison with PE from sage which present high inhibition of *E. coli* 0157H7 hemagglutination but low activity in *E. coli* 0157H7 agglutination (Table 5).

The PE from rue causes a poor agglutination (14 units of *E. coli* 0157H7 agglutination), however our outcomes evidenced high cytotoxic effect and crystal formation determined by microscopy observation with both sage and rue PE. It is necessary to consider that the greater part of the PE showed high HA in blood type B, which means Gal and GalNAc recognition also and hemolytic protection effect against Neu5Ac and GlcNAc sugars in unwashed blood samples.

Activity from fruits PE in the adhesion of *E. coli* 0157H7 bacteria and their toxicity to HELA cells

In about 100 HELA cells analysed most PE after 2 hrs in the presence of the bacteria were highly toxic (100-70%), such as rue, chamomile, dayflower, fennel, sage, melisa arnica, and in the case of mint, guava, wormseed, tropical bushmint and horehound were less toxic around 30% similar to the toxicity to the cells of the bacteria per se (Table 6). The number of bacteria on the cells that were identified, with arnica, chamomile fennel and wormseed was around 20-30 bacteria/per cell, similar to the control, in the others PE were around 5-15 bacteria /per cell and in the case of sage, rue and horehound, bacteria were not identified because only crystals were find.

Discussion

As expected, we detected lectin activity in all PE and suggest that at least two or more types of lectins recognized glycoside determinants in the membranes of the erythrocytes such as Gal, GalNAc, Man, Gluc, GlucAc, and Neu5Ac. Also, all PE showed a better recognition of blood type B, suggesting the presence of lectins, mainly related to Gal or it is derivates as GalNAc, GalN may be a Gal/GalNAc type lectin; even those PE from different families.

The PE with high specificity were Tropical bush mint, dary flower, sage, wormseed, arnica, mint, and chamomile, which inhibited *E. coli* 0157H7 hemagglutination activity in all blood types A, B and O, as well as *E. coli* 0157H7 agglutination. Those data suggest that recognition may occurs by some antigenic determinant in the microorganism or common sugars in erythrocytes, such as Neu5Ac, Gal present in TN, M antigenic in the case of erythrocytes, [31] or Gal/GalNAc and Neu5Ac antigens from bacteria [30,31].

According to the results from the agglutination of *E. coli* 0157H7, lectins from PE shown more specificity to some bacterial antigen determinants such as fimbriae type 1 (Man), S (Neu5Ac) or P, (Gal/GalNAc) because they are involved in adhesion [22,32,33]. When we explored the sugar recognition specificity of lectins from bacteria, erythrocyte or PE, we found that is required different quantities of sugars for HA and inhibition of *E. coli* 0157H7 hemagglutination.

The quantity of each sugar varies significantly depending on blood type and PE. We propose these results towards two mechanisms of adhesion: the first one, those responsible for carbohydrate domain recognition (CDR) in the lectins and the glycosidic signal, which means, a protein-sugar interaction that could be involved in trigger some catalytic activity that can remove the glycosidic signal and be more specific; second one, those that are not well known or established, for example, adhesion interaction between glycosidic chains in both erythrocytes and lectins, either from the microorganism or PE.

This sugar-sugar interaction could be done by hydrogen bridge between the hydroxyls (OH), that requires greater sugars quantities to break this molecular binding as compared to low amount needed in the CDR protein-sugar interaction. Also, the effects of some secondary metabolites such as phenolic derivatives (flavonoids and lignans) that contain large number of OH, could compete with the sugars involved in adherence between bacteria and the host tissue and act as natural antiadhesive [33].

Although sugar-sugar interaction could be product of unspecific binding and may require some kind of orientation about OH⁻ atoms of sugars involved, may be why high molar concentrations of sugars such as Glc, Xyl Man and Fuc showed an inhibition of hemagglutination *E. coli* 0157H7 in blood groups 3.

This may apply mannose and glucose sugars strongly were recognized in most PE in blood type B and involved in lectin activity, HA, hemagglutination inhibition and agglutination of *E. coli* 0157H7, give us a better understanding of the results. The mechanism of adhesion used by bacteria could be explained by the high specificity of PE to inhibit *E. coli* 0157H7 hemagglutination in all blood types and by *E. coli* 0157H7 agglutination. The hemagglutination specificity for blood type B, the similar inhibition of *E. coli* 0157H7 HA in blood types A, B or O and also the agglutination of *E. coli* 0157H7 by the PE, suggest basically a recognition to a determinant antigenic from the microorganism, such as lipopolysaccharide (LPS), O antigen or, fimbrial type 1 or P or S [32,20,33], and also to some common sugar from the erythrocytes such as Neu5Ac; Gal present in TN and M antigenic in erythrocytes[32].

However, the effect of the PE in the *E. coli* activities, principally P Fimbriae type P are involved, because plants PE's that inhibited the EcAg and the EcHA recognized Gal / GalNAc. In this work we use the PE from rue as negative control, because it is particularly used as abortive, but few reports revealed their gastrointestinal activity, however we show that rue and sage PE were highly cytotoxic to bacteria and HELA cells, this may explain the low *E. coli* 0157H7 agglutination observed in those PE, basically it was watching crystals formation.

The cytotoxic effect may involve amine sugars recognition by rue and sage PE, such as GlcN and GalN, besides Neu5Ac lectins, present in bacterial fimbriae associated to porins [3,10] or through RIP type lectins with highly toxic effect, both with 30 kDa band [27, 26, 34,35]. Concerning to HA activity from PE of plants, most of them have lectin which recognized with the same specificity glycosides determinant from group A, B and O, which also involved in their activity in the inhibition of the *E. coli* 0157H7 HA.

On the contrary PE from tropical bushmint, dayflower showed highly *E. coli* O157H7 agglutination, and fennel and horehound showed only be more specific to it that means that have a lectins that recognized better the *E. coli* O157H7, and respect the sugar involved in those activities, probably are acylated derivates sugars (GalNAc, Neu5Ac, GlcNAc), also for the first time that Xyl is founded involve in those activities. About protein band pattern, most of the PE showed a common bands, all PE showed a 14 kDa band that may be Monocot lectin and 17-18 kDa band possibly a (Chi) type lectin [36,37].

Rue and dayflower showed different bands, around 30 kDa and PE from sage, melissa, arnica, mint and wormseed displayed bands of 30-40 kDa, these may be a RIP type lectin, or some lectin derivates without cytotoxic effect, such as B-rycin reported for *Sambucus nigra*[34].

We found proteins similar to albumin migration in PE from melissa, guava and sage also with high molecular weight over 100 to 257 kDa, probably molecular aggregates a consequence of the extraction conditions mainly to low salt. Our results suggest in the majority of the PE at least two or three types of lectins with bands pattern around 14, 18, 20 and 28 kDa; a molecular weight that may belongs to Monocot (Man), Chi (GlcNAc), B-ricin or RIP (GalNAc/Neu5Ac) lectins [34-37].

Which are implicated in some of the activities studied in *E. coli* O157H7 enterohemorrhagic such as hemagglutination, agglutination and toxicity, probably RIP, CHI and Gal/GalNAc type lectins are the implicated by it is toxic effect en HELA cells that could be necrotic apoptotic effect and also lectins that recognized GalN and GlucN in the toxicity to bacteria, and these toxic effect do not allowed determinates cells adhesion.

Ribosome inactivating proteins lectins recognized GalNAc/Neu5Ac, are involved in apoptosis as most PE from plants has a cytotoxic effect in HELA cells. and also recognized Gal/GalNAc, probably are RIP lectin and the cytotoxic effect basically depend in a Gal recognition through the apoptotic death FAS/CD95 receptor, those death receptor galectin depend on calcium and is associated with the independent caspase-3 of mitochondria inducing apoptosis in lymphocyte also this second apoptotic pathway (extrinsic pathway) triggered necrosis after the binding to death receptors, may induces activation of proteolytic enzymes such as, caspases; that in turn activate endonucleases, all mediated by bcl-2 proteins, which regulate mitochondrial permeabilization processes and induce apoptosis or necrosis because granzymes proteases that induced the pore formation and lysis are also activated through death FAS/FasL receptor (38). The pore formation may be also activated by the GlcNAc recognition by Chi type lectins because chitin recognition also is involved in apoptosis (38,39,40).

The high cytotoxic effect of plants PE to HELA cells and to *E. coli* activities may be due to a synergistic effect of more than two lectins involved in the different effects, which for the sugars recognition and for the pattern of bands could be Chi, Gal/GalNAc or RIP type lectin (27,34,38,39,40). However, it most possible to be dealing with leguminosea type lectins too, because they recognize several complex sugars and also Xyl lectin, as xylose was found to participate in HA and in the EcHA and probably in *E. coli* agglutination and toxicity to HELA cells, this suggests proteoglycan participation in adhesive and toxicity mechanisms (41).

The use of teas or tizanas from plants can give protection against some pathogenic factors of enterohemorrhagic *E. coli* O157H7 [25] and can prevent diseases, and others, such as viral infections.

Previous reports has shown that Man, GlcNAc lectins are selective and powerful inhibitors of human deficiency virus and cytomegalovirus replication *in vitro*[42,43]. In addition, several enterobacteria such as *Vibrio cholerae*, *Shigella* and *Salmonella* share antigenic determinants and pathogenic factors with *E. coli*. [18,22, 44]. The use of PE above mentioned may counteract the effects of those bacteria as well as the *E. coli* O157H7. In Mexico the common use of alternative medicinal plants could be a reason why in México, *E. coli* O157H7 is not a public health problem as it is in the USA or some Latin-American countries such Argentina and Chile that consume uncooked swine meat and cattle which are also *E. coli* O157H7 reservoir [6].

Our and other studies support the use of lectins as active compounds to control bacterial infections and there are useful markers in order to study cellular growth, also can be used in malignancy diagnostic, in prognostic and tumor treatment because type RIP I and II lectins which have apoptotic or necrotic death [26,27,28, 34,38,39,45].

However, we must be discrete using plants and other natural sources for treatments, because in the case of lectins they recognize specifically red cell groups and agglutinate them or even caused hemolysis of red cell. This may cause not only an immunological response, but also, a renal disease. We consider that each treatment or preventive care must be customized considering lectins capacity to recognize some sugars present in specific blood type but also specific for sex, because in preliminary studies in PE from mango (*Mangifera indica*) (Maria Carmen Arenas 2005)[46], and other PE from *Eichornia crassipens* and *Lemna minor* (no published Data) was detected lectins from those that are specific to sex recognition for group A and O.

Finally, in the almost 100 years of lectins studies our studies summarized to it was shown, that they play an important role as recognition molecules in cell-molecule, and cell-cell interactions in a variety of biological systems (47) even it is importance in molecule-molecule interaction which are usefully to understand cell regulation process such as necrotic and apoptotic by the FAS receptor and lectins type RIP and CHI [38,40,46].

Ethnomedicine, is an integral part of the culture and the interpretation of health by indigenous populations in many parts of the world. Mexico has an ancestral traditional Ethnomedicine knowlege[29], some of the bioactives found in these fruits, plants and marine organism are secondary metabolites such as alkaloids, flavonoids, phenolic compounds , tannins etc, and another could be primary metabolites such several proteins with lectin activity and inclusive peptides, vitamins, minerals and carbohydrates which are involved in the therapeutic activities.

This Ethnomedicine knowledge is very important to maintain, for treatments and curing of current ailments, especially for the extensive and abusive use of antibiotics and synthetic chemicals that has brought an increase of bacteria resistant to drugs, and an increase in neoplastic processes (28, 48,49,50).

Acknowledgments

This study had financial support from SIGOLFO 97-02-003 grant. The authors also wish to thank to the evaluation committee from SIGOLFO and specially Dr. Emilio Pradal Roa and Jorge Papacristofilos, regional coordinators, for their comments on this work. The authors also wish to thank Mr. Warren Haid, Marquina and Irene Xochihua Rosas for proof-reading review.

References

- [1]Griffin, P.M.; Tauxe, R.V. The epidemiology of infections caused by *Escherichia coli* O157:H7, other enterohemorrhagic *E. coli*, and the associated hemolytic uremic syndrome. *Epidemiol. Rev.* 1991, 13: 60-98.
- [2]O'Brien, A.D.; La Veck, G.D.; Thompson, M.R.; Fomral, S.B. Production of *Shigella dysenteriae* type 1-like cytotoxin by *Escherichia coli* *J Infect Dis.* 1982, 146: 763-769.
- [3]Rivero, M.A.; Padola, N.L.; Etcheverria, A.I. Parma, A.E; *Escherichia coli* enterohemorrágica y síndrome urémico hemolítico en Argentina. *Medicina (buenos Aires).* 2004, 64: 352-356.
- [4]Margall, N.; Dominguez, A.; Prats, G.; Salleras, L. *Escherichia coli* enterohemorrágica *Rev Esp Salud Pública.* 1997, 71: 437-443.
- [5]Lopez, E.L.; Diaz, M.; Ginstein, S.; Devoto, S.; Mendilaharsu, F.; Murray, B.E.; Hemolytic uremic syndrome and diarrhea in Argentine children: the role of Shiga-like toxins. *J Infect. Dis* 1989, 160: 469-475.
- [6]Borie, C.; Monreal, Z.; Guerrero, P.; Sanchez, M.L.; Martínez, j.; Arellano, C.; Prado, V. Prevalencia y caracterización de *Escherichia coli* enterohemorrágica aisladas de bovinos y cerdos sanos faenados en Santiago, Chile., *Arch. med.* 1997 *vet.* 29: 205-212.
- [7]Levine, M.M. *Escherichia coli* that cause diarrhea: enterotoxigenic, enteropathogenic, enteroinvasive, enterohemorrhagic, and enteroadherent.. *J Infect Dis.* 1987, 155, 377-89.
- [8]Karch H, Heesemann J, Laufs R, O'Brien AD, Tacket CO, Levine MM A plasmid of enterohemorrhagic *Escherichia coli* O157:H7 is required for expression of a new fimbrial antigen and for adhesion to epithelial cells. *Infect Immun.* 1987, Feb;55(2):455-461
- [9]Klaus, J.; Barbara, J. *Can.J. Microbiol.* Capsules of *Escherichia coli*, expression and biological significance 1992, 38, 705-710.
- [10]Hacker, J. Role of fimbrial adhesins in the pathogenesis of *Escherichia coli* infections *Can. J. Microbiol.* 1992, 38, 720-727
- [11]De Graaf, F.K. The fimbrial lectins of *Escherichia coli*. In *Lectins , Biology, biochemistry, clinical biochemistry,* Vol. 5 , Ed Walter de Gruyter & Co., Berlin- New York Berlin Germany; 1986, pp 285-296
- [12]7. Duncan, S.H.; Scott K.P.; Flint H.J.; Stewart, C.S. *Comensal –Pathogen Interactions involving E coli 01576 and the prospects for control Genetic and Molecular Ecology of Escherichia coli.* In *Escherichia coli in Farm animals* ed C.S. Stewart and J Flint H.J. published by CABI publishing New York, USA; 1999, pp 71-89
- [13]Durno, C.; Soni, R.; Sherman, P. *Clin Invest Med.* 1989, 12, 194-200
- [14]Nataro, J.P.; Kaper, J.B. Diarrheagenic *Escherichia coli*. *Clin Microbiol Rev.* 1998, 11, 142-201
- [15]E. Van Driessche, et all. Enterotoxigenic fimbrial *Escherichia coli* lectins and their receptors: targets for probiotic treatment of diarrhoea: Arpad Pusztail and Susan Bardocz (eds) *Lectins, Biomedical Perspectives ,* Taylor & Francis London WC1N2ET ,UK; 1995 pp 235-292.
- [16]Rodriguez-Angeles, G. *Salud Pública de México.* 2002, 44, 464-475
- [17]Mouricout, M.; Vedrine, B. *Lectin-Carbohydrate Interactions in Bacterial Pathogenesis* In: *Lectins and Pathology.* Ed. Michael Caron and Annie-Pierre Save published by Harwood Academic publishers. Amsterdam Netherlands; 1999 pp169.

- [18] Merrit, E.A. Mol. Microbiol. 1994, 13, 745-753
- [19] Doyle, R.J. Introduction to Lectins and their Interactions with Microorganisms- R. J. Doyle and Malcom Slifkin, Marcel Dekker (Eds) Lectin-Microorganism Interactions. US: Marcell Dekker; 1994. pp 1-8
- [20] Shakanina K.I and Kalinin N.L. Microbial Lectin for the investigation of glycoconjugates. In: Ed Doyle, R Malcom Slifkin. Lectin Microorganism Interactions. US Marcell Dekker; 1994. pp299-326
- [21] Sharon, N.; Lis, H. Bacterial lectins and biological perspectives of lectins In Lectins properties, function and application in biology and medicine, New York Academic Press; 1986, pp 494, 2266
- [22] Coutiño-Rodríguez, R.; Hernandez-Cruz, P.; Giles-Ríos, H. Lectin in fruits and their participation in the hemagglutinating activity of *E. coli* O157H7 Archives of Medical Research 2001, 32, 251-257.
- [23] Slifkin, M. Application of Lectins in Clinical Bacteriology. Ed. Pusztai A and Bardocz S Lectins, Biomedical Perspectives Taylor & Francis UK; 1995.
- [24] Plant Lectins: A special class of plant proteins. In. Handbook of Plant Lectins: Properties and Biomedical Applications. Ed J.M Van Damme, Willy J. Peumans, Pusztai Arpad and Bardocz Susan published by John Wiley & Sons England, London U.K. WIP9HE; 1998
- [25] Hirno, S.; Utt, M.; Wadstöm, T. Sialylglycoconjugate and proteoglycan-binding microbial lectins: In Lectins, Biology,
- [26] Biochemistry, Clinical Biochemistry, Vol. 12. Ed Edilbert Van Driessche, Sonia Beeckmans and Thorkild C. Bog-Hansen published by TEXTOP DK-2900 Hellerup, Denmark, ISBN 87-984583-0-2; 1997
- [27] R Hartley and J.M Lord. Cytotoxic ribosome-inactivating lectins from plants. M. Biochimica et biophysica Acta (BBA)- Proteins and Proteomics. 2004(1701) Issues 1-2 pag 1-14
- [28] Sriram Narayanan, Kalpana Surendranath, Namrata Bora, Avadhesin Surolia, Anjali A Karande Ribosome inactivating proteins and apoptosis. <http://sciencedirect.com/science/article/pii/S0014579305001274>
- [29] Bo Lui, He-Bian. Jin.Ku Bao Plant lectins: Potentially antineoplastic drugs from bench to clinic. Cancer Letters 2010; 267 Issue 1, pag 1-2
- [30] Lozoya, J.; Aguilar, A.; Camacho, J.R. Encuesta sobre el uso actual de las plantas en la Med. Tradic Mexicana Rev. Med. IMSS (Mex). 1987, 25, 273:283.
- [31] Evans, D.J.; Evans, D.G.; Young, L.S.; Pitt. J. Hemagglutination typing of *Escherichia coli*: definition of seven hemagglutination types. J. Clin. Microbiol. 1980, 12, 235-242
- [32] Fukuda Minoru Ole Hindsgaul. Cell Surface Carbohydrates: Cell Type specific expression in Molecular Glycobiology. Ed. IRSL PRESS: New York; 1994
- [33] Melnicktz, J.; Adelbergs. 18a ed traducida de la 23 ed en Ingles Geo Brooks, Janet S Butel, Stephen A Morse. Janet Melnicktz and Adelbergs editor Microbiología Médica Manual Moderno, Estructura celular 2005, pp 9-40
- [34] Dhiraj A Atterm, Reza Ghaedian, Kalidas Shetty. Enhancing health benefits of berries through phenolic antioxidant enrichment. focus on cranberry Asi.Pac.J. Clin Nutr. 2005;14(2):120.

- [35]Van Damme E.J, Roy S., Barre A, Citores L., Mostafapous K., Rouge P, Van Leuven F, Girbes T, Goldstein I.J, y Peunams W J. Elderberry (*Sambucus nigra*) Bark contains two structurally different Neu5Ac(α 2,6) Gal/GalNAc-binding type 2 ribosome-inactivating proteins. *Eur.J. Biochem.*1997; 245(83):648-655.
- [36]Barbieri, L.; Battelli, M.G.; Stirpe, F. *Biochemical and Biophysics Acta.* 1993. 1154: 237-282.
- [37]Barre Annick, Els J.M. Van Damme, Willy J. Peumans, and Pierre Rougé. Structure-Function Relationship of Monocot Mannose-Binding Lectins *Plant Physiology.* 1996; 112:1531-1540.
- [38]Collinge, D.B.; Kragh, K.M.; Mikkelsen, J.D.; Nielsen, K.K.; Rasmussen, U.; Vad, K. *Plant Journal.* 1993, 3: 31-40.
- [39]Luis Alfredo Herbert Doctor, Elda Ma. del Rocío Coutiño Rodríguez, Beatriz Palmeros-Sánchez, y Clara Luz Sampieri Ramírez. "Necrotic and Apoptotic Activity of the Protein Extract from *Mangifera indica* Mesocarp in Human Lymphocytes in Culture" *Econfar Journal Bolivia* June 2017; 4(6) 28-47 ISSN 2007-1582, e-ISSN: 2007-3682 682.
- [40]Yu Koyama, Yuko Katsuno, Noriyuki MIYOSHI, Sumio Hayakawa, Takashi Mita, Harohitko Muto, Yuktaka Aoyagi, and Mamoru Isemura Apoptosis induction by lectin isolated from the mushroom *Boletopsis leucomelas* in U937 cells *Biosci., Biotechnol,Biochem* 2002 66(4); 784-789
- [41]Malathi Srilakshmi Vakkalanka, Evaluating Structural different pectic oligosaccharides in inhibiting adhesion of *E coli* 0157H7 to human gut epithelial cells in vitro Thesis in Master of Science Graduate Program in FOOD Science University of New Jersey 2013 October
- [42]Qinghong Liu, Hexiang Wang, T.B. Ng Qinghong Liu, Hexiang Wang T.B. First report of a xylose-specific lectin with potent hemagglutinating, antiproliferative and anti-mitogenic activities from a wild ascomycete mushroom. *Biochimica et Biophysica Acta* 1760 (2006) 1914–1919
- [43]Balzarini, J.; Neyts, J.; Schols, D.; Hosoya, M.; Van Dame, E.; Pneumans, W.J.; De Clercq, E. *Antiviral Res.* 1992, 18: 191-207. Balzarini, J.; Neyts, J.; Schols, D.; Van Dame, E.; Pneumans, W.J.; De Clercq, E. *Antimicrob Agents Chemother.* 1991, 35: 410-416.
- [44]Coutiño-Rodríguez, R.; Giles, R.H. Lectinas de plantas en los procesos adhesivos microbianos En *Neuroetología la década del cerebro y la conducta animal.* Jorge Manzo Denses Eds. Instituto de Neuroetología Universidad Veracruzana ISBN-968-834-588-1, 2002; pp 149-164.
- [45]Tandehui Belem Gallegos, Rocio Coutiño, Gisela Martínez y Pedro Hernández Cruz. Marcadores Glicosidados en cáncer de mama. *REB* 2008, 27(2):52-59 ISBN 1665-1995
- [46]Nathan Sharon and Halina Lis. History of lectins: from hemagglutinins to biological recognition molecules. *Glycobiology.* 2004 14(11): 53R-62R
- [47]Maria del Carmen Arenas y Rocio Coutiño Rodríguez. Protein extracts with lectin activity of *Mangifera indica* L. show sex-dependent differences in hemagglutination of blood groups A and O presentado en XI Congreso Nacional de Bioquímica y Biología Molecular de Plantas y 5° Simposium México EUA. Del 3 al 7 de Nov. Del 2003 en Acapulco Guerrero, pg 294
- [48]G.B Mahady Medicinal Plants for the Prevention and Treatment of bacterial infections :*Current Pharmaceutical design* 2005, 11(19)

[49]Alejandro M.S Mayer and Mark T. Hamann Marine pharmacology in 2001-2002: Marine compounds with antihelmithic, antibacterial, anticoagulant, antidiabetic, antifungal, anti-inflammatory, antimalarial, anmtiplatelet, antiprozoal, antituberculosis, and antiviral activities, affecting the cardiovascular, immune and nervous systems and other miscellaneous mechanisms of action. Comparative Biochemistry and Physiology Part C 140, 2005, pp 265-286.

[51]Supayang Piyawan Voravuthikunchai and Hazel Mitchell Inhibitory and killing activities of medicinal plants against multiple antibiotic-resistant helicobacter. Journal of Health Science;2008,54(1)81-88

Annexes

Scientific name (Common name)	Family	Uses	Protein (mg/mL)	Carbohydrate (µg/mL)
<i>Hyptis mutabilis</i> (Tropical bush mint)	Lamiaceae or Labiataceae	I	0.50	0.06
<i>Zebrina pendula</i> (dayflower)	Commelinaceae	I, II	0.32	0.12
<i>Salvia officinalis</i> (sage)	Lamiaceae	II, III	0.505	0.17
<i>Chenopodium ambrosoides</i> (wormseed)	Chenopodiaceae	III	2.11	0.15
<i>Heteroteca indulis</i> (arnica)	Compositae or Asteraceae	III	2.18	0.355
<i>Mentha piperita</i> (mint)	Lamiaceae or Labiataceae	I, II, III, IV	0.635	0.125
<i>Matricaria chamomilla</i> (chamomilla)	Compositae or Asteraceae	II, III, IV	2.52	0.085
<i>Melissa officinalis</i> (melissa)	Lamiaceae or Labiataceae	III	0.65	0.198
<i>Foeniculum vulgare</i> (fennel)	Umbelliferae	III	1.46	0.365
<i>Marrubium vulgare</i> (horehound)	Lamiaceae or Labiataceae	II, IV	2.18	0.54
<i>Psidium guajava</i> (guava)	Myrtaceae	I, II, III	1.26	0.42
<i>Ruta xalapensis</i> (rue)	Rutaceae	II, III, IV	0.775	0.12

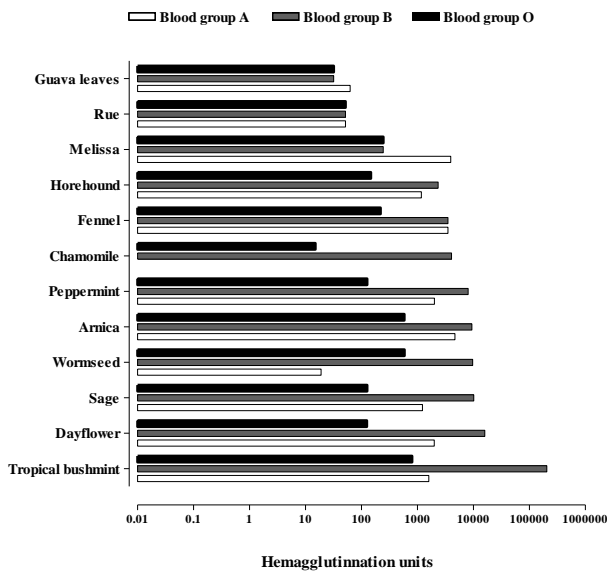


Figure 1 Characterization of hemagglutination activity from PE in each blood type. Hemagglutination activity (HA) of PE was carried out as described in material and methods in different male blood type A, B or O. The HA is reported as HA units (titer x dilution factor)/protein concentration. The agglutination of erythrocytes, based on a control, was taken as a positive control

Table 1 Plants classifications and concentration of proteins and carbohydrates. Classification of plants was according to the ethnobotanical studies and by surveys by IMSS COPLAMAR, Javier Lozoya, 1987. I, antidiarrheal; II, antidyseritic; III, antiparasitic; IV, antiamoebic. Protein and carbohydrates quantification as described in material and methods

Common name	Protein titer (mg/mL)	Blood type	Sugars type concentration
Tropical bushmint	0.005	A B O	Xyl, GalNAc (15µM) Man, Glc, GalNAc, Fuc (15µM) Gal, GlcNAc (15µM)
Sage	0.05	A B O	Gal, GlcNAc, GalNAc, GalN (31µM) Man, Glc, GalNAc (15µM), Neu5Ac (15µM) Xyl, (31µM)
Wormseed	0.13	A B O	Glc, Gal (15 µM), GlcNAc (31µM) Glc, Fuc, Gal, (15µM) Glc, Man (15µM) GINAc and Xyl (31µM)
Arnica	0.017	A B O	Xyl, GalNAc (62µM) GalNAc, Neu5Ac (62µM) Gal (125µM)
Mint	0.079	A B O	GalNAc, GlcN, Neu5Ac, Man and GalN (15µM) Glc, Man GlcN, Fuc (15µM) Fuc, GlcNAc, GalNAc Neu5Ac and Xyl (15µM)
Chamomile	0.078	A B O	ND Fuc, Neu5Ac (15µM) Fuc (15µM)
Fennel	0.36	A B O	Man, Glc, GlcN, Xyl (15µM) Man, Glc, GalNAc, Fuc (15µM) Man GalNAc (15µM)
Dayflower	0.01	A B O	Man, GlcNAc, GalNAc, GalN (31µM) Neu5Ac (31µM) Neu5Ac (31µM)
Horehound	0.55	A B O	Man, Gal, GlcN, GlcNAc, GalNAc, Neu5Ac and Xyl (15µM) Gal, GlcNAc (15µM) Man, GlcNAc, GalNAc, Neu5Ac and Xyl (15µM)
Melissa	0.65	A B O	Gal, GalN, Neu5Ac (15µM) Man, GlcNAc GalNAc, Glc, GalN (15µM) Man and Fuc (15µM)
Guava leaves	1	A B O	Glc (15µM) Neu5Ac, Man, Glc, and Gal (15µM) Man, Gal, Xyl, Fuc, GalN and Neu5Ac (15µM)
Rue	0.775	A B O	GlcN (31µM) Man, Glc, GalNAc, GalN, GIN, Neu5Ac (15µM) Neu5Ac (15µM)

Table 2 Common Sugars that inhibiting the HA caused by PE in each blood group. The lectins specificity was determined by HA competition with sugar standards at 0.015 at 1mM and with double serial dilutions using titer with lower protein concentrations from each PE that induces HA (see material and methods)

EXTRACT	Relative molecular weight (kD)								
Horehound	257					25	18	17	
Sage		160	98	71	47	30, 34, 37		18,17	14
Melissa		164	89	69		35	20, 23	18, 16	14
Tropical bushmint	257						20	18,17	15
Mint	238		112		58	33	20, 28	18	
Arnica	245	167	112	88	53	32, 34, 41	20	18,	16
Chamomile	250						20	18,17	15
Wormseed	246				56	39, 43	21, 20	17	14
Fennel						46	20	18	17
Rue						30	22,20,	19	
Dayflower	264				58		21	19, 18	14
Guava leaves	264			60			21	19	17
Weight marker (GIBCO)	194	120	87	64	52	39	26	21	15

Table 3 Protein electrophoretic mobility from PE. Proteins from PE were resolved in 10% SDS-PAGE as described in material and methods. The results were obtained with autoanalyzer and Digital MSD 40 Kodak Program using standard proteins pre-stained weight marker(GIBCO)

Sugars	Type A	Type B	Type O
Neu5Ac	125 µM	1 mM	15 µM,
GlcNAc	15 µM, 250 µM	15µM	62 µM, 10mM
GalNAc	125 µM, 10mM	31µM	250 µM, 1mM
Gal	250 µM, 15µM,	250	62 µM, 250 µM
Gal N	15 µM, 125 µM	µM, 10mM	62 µM,
Glc	250 µM	250 µM,	15µM, 250 µM,
GlcN	250 µM, 1mM	15 µM,	,
Xyl	1mM, 10 mM	1mM, 10mM	62 µM, 125 µM,
Fuc	1mM, 10 mM	1mM	10 mM
Glc	1mM	1mM	1mM, 10 mM
Man	1mM, 10mM	1mM	1mM
		1mM	1mM, 10 mM
			ND

Table 4 Sugars that inhibit HA of E. coli 0157:H7. The HA assay was as described in material and methods. The standard sugars were diluted (10mM to 1 M), double serial dilutions was done to get the minimum amount of sugar able to inhibit the E. coli HA

Common name	HA group B (HA units)	<i>E. coli</i> 0157:H7 HA inhibition (specific activity)	<i>E. coli</i> 0157:H7 agglutination (specific activity)
Tropical bushmint	204800	102400 A,B,O	26841
Dayflower	16000	16000 A,B,O	14755
Sage	10139	10137 A,B,O	265
Mint	8063	8063 A,B,O	7367
Melisa	246	7877 A,B,O	2897
Rue	52	6006 A,B	14
Guava leaves	32	4063 A,B,O	667
Fennel	3507	3505 A,O	6918
Wormseed	9706	2426 A,B,O	129
Horehound	2347	2349 A,B,O	19033
Chamomile	4063	2031 B	603
Arnica	9706	1174 A	1280

Table 5 Effect of PE in the HA of blood group B, in *E. coli* HA Inhibition and *E. coli* agglutination. Hemagglutinating units was calculated as (titer x dilution factor)/protein concentration. The Specific activity of *E. coli* 0157:H7 HA inhibition was (titer) minimum for perceiving *E. coli* 0157:H7 HA x dilution factor (g of protein from PE). Specific activity of PE of *E. coli* 0157:H7 agglutination was calculates as *E. coli* 0157:H7 agglutination x dilution factor (40)/(g of protein from PE)

Samples extracts	Cytotoxic Effect (A)	Number of bacteria present after 2 hours(B)	Number of bacteria present after 24 hours(C)
Rue	100	0 crystals	0
Chamomile	90	25	5 small colonies
Dayflower	83	5	Dot colonies
Fennel	88	20	Dot colonies
Sage	80	0 crystals	Dot colonies
Melisa	80	5	Dot colonies
Arnica	70	30	0
Wormseed	35	20	Dot colonies
Tropical bush mint	30	15	0
Mint	20	5	1 big and dot colonies
Guava	15	10	Dot colonies
Horehound	5	0 crystals	0
Cells with bacteria	25 and 1% anuclei cells	30	5 regular colonies
cells	10	0	0

Table 6 Effect of the PC on adhesion of HELA cells in *E. coli* 0157:H7 presence. A; % of toxicity of HELA cells in the presence of bacteria and PE for 2 hrs. B; % of bacterias showing adhering or internalized after 2 hrs in the presence of PE. C;% of bacteria colonies after 2 hrs in the presence of PE in HELA and two washings with PBS, nutritive agar was added to the cells and they were incubated for 24 hrs, after which the units forming colonies (UFC) were counted.

Instructions for authors

[Title in Times New Roman and Bold No.14]

Last name -First name, (in uppercase) -1st † Last name -First name (in uppercase) -2nd Author's name

Institutional mail No.10 Times New Roman and Italic

(Report Submission Date: Month, Day, and Year); accepted (Insert date of Acceptance: Use Only ECORFAN)

Abstract

Title

Objectives, methodology

Contribution

(150-200 words)

Keywords

Indicate (3-5) keywords in Times New Roman and Bold No.11

Citation: Last name -First name (in uppercase) -1st † Last name -First name (in uppercase) -2nd Author's name. Paper Title. Title of the Journal. 2016 1-1: 1-11 - [All in Times New Roman No.10]

† Researcher contributing as first author.

Instructions for authors

Introduction

Text in Times New Roman No.12, single space.

General explanation of the subject and explain why it is important. What is your added value with respect to other techniques?

Clearly focus each of its features

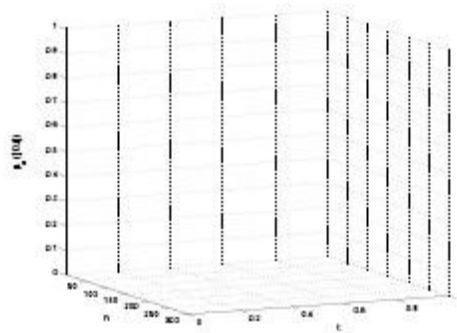
Clearly explain the problem to be solved and the central hypothesis. Explanation of sections Article.

Development of headings and subheadings of the article with subsequent numbers

[Title No.12 in Times New Roman, single spaced and Bold] Products in development No.12 Times New Roman, single spaced. **Including graphs, figures and tables-Editable**

In the article content any graphic, table and figure should be editable formats that can change size, type and number of letter, for the purposes of edition, these must be high quality, not pixelated and should be noticeable even reducing image scale.

[Indicating the title at the bottom with No.10 and Times New Roman Bold]



Graphic 1 Title and Source (in italics).

Should not be images-everything must be editable.

Instructions for authors

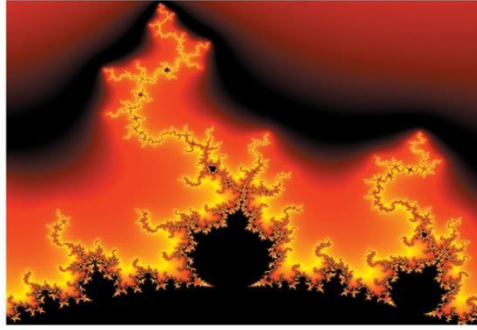


Figure 1 Title and Source (in italics).

Should not be images-everything must be editable.

Table 1 Title and Source (in italics).

Should not be images-everything must be editable.

Each article shall present separately in **3 folders**: a) Figures, b) Charts and c) Tables in .JPG format, indicating the number and sequential Bold Title.

For the use of equations, noted as follows:

$$Y_{ij} = \alpha + \sum_{h=1}^r \beta_h X_{hij} + u_j + e_{ij}$$

(1)

They must be editable and number aligned on the right side.

Methodology

Develop give the meaning of the variables in linear writing and important is the comparison of the used criteria.

Results

The results shall be by section of the article.

Annexes

Tables and adequate sources thanks to indicate if they were funded by any institution, University or company.

Instructions for authors

Conclusions

Explain clearly the results and possibilities of improvement.

References

Using APA system, should **Not** be numbered, either bulleted, however, if necessary, will be because reference number or referred to in any of the article.

Data Sheet

Each article must submit your dates into a Word document (.docx): Journal Name

Article title

Abstract

Keywords

Article sections, for example:

1. *Introduction*
2. *Description of the method*
3. *Analysis from the regression demand curve*
4. *Results*
5. *Thanks*
6. *Conclusions*
7. *References*

Author Name (s)

Email Correspondence to Author

References



ECORFAN®

Santa Elena, Ecuador _____, _____ 20_____

Originality Format

I understand and agree that the results are final dictamination so authors must sign before starting the peer review process to claim originality of the next work.

Article

Signature

Name



ECORFAN®

Santa Elena, Ecuador _____, _____ 20_____

Authorization form

I understand and accept that the results of evaluation are inappealable. If my article is accepted for publication, I authorize Ecorfan to reproduce it in electronic data bases, reprints, anthologies or any other media in order to reach a wider audience.

Article

Signature

Name

ECORFAN Journal-Ecuador

“Energy potential of some forest species in the northern zone of the Yucatan Peninsula, for their use as solid fuels”

AGUILAR-SÁNCHEZ, Patricia, CARRILLO-ÁVILA, Noel, SUÁREZ-PATLÁN, Edna Elena, ORDÓÑEZ-PRADO, Casimiro.

“The ferrite nanoparticles (Fe_2O_3) impact on germination, growth and lignine content of carrot (*Daucus carota*)”

VALLE-GARCIA, Jessica Denisse, VAZQUEZ-NUÑEZ, Edgar and CASTELLANO-TORRES, Laura Edith

Universidad de Guanajuato

“Synthesis and characterization of Pd/TiO₂ thin films with possible applications in photocatalysis”

TIRADO-GUERRA, Salvador and VALENZUELA-ZAPATA, Miguel

“Renewable energy potential in the Usumacinta watershed: Status and opportunities”

PAMPILLÓN-GONZÁLEZ Liliana, SARRACINO-MARTÍNEZ Omar, HERNÁNDEZ-GÁLVEZ Geovanni, ORDAZ-FLORES Alejandro

Universidad Juárez Autónoma de Tabasco

Universidad Iberoamericana

“Lectins Gal/GalNAc from medicinal plants extracts with gastrointestinal activity have effects on the biological activity of *Escherichia Coli* O157H7”

GILES-RIOS, Héctor, COUTIÑO-RODRIGUEZ, Rocío, ARROYO-HELGUERA, Omar, HERNÁNDEZ-CRUZ, Pedro

Universidad Veracruzana.

UNAM-UABJO

